FLOOD HAZARD MODELING AND RISK MAPPING: CASE STUDY ON LOWER WEITO RIVER RIFT VALLEY BASIN SNNPR, ETHIOPIA.

M.Sc. THESIS

GELMA BORU

HAWASSA UNIVERSITY HAWASSA, ETHIOPIA

FLOOD HAZARD MODELING AND RISK MAPPING: CASE STUDY ON LOWER WEITO RIVER RIFT VALLEY BASIN SNNPR, ETHIOPIA.

GELMA BORU

A THESIS SUBMITTED TO THE
FACULTY OF BIO-SYSTEMS AND WATER RESOURCE ENGINEERING
DEPARTMENT OF HYDRAULIC AND WATER RESOURCE ENGINEERING
HAWASSA UNIVERSITY INSTITUTE OF TECHNOLOGY, SCHOOL OF GRADUATE STUDIES
HAWASSA UNIVERSITY
HAWASSA, ETHIOPIA
IN PARTIAL FULFILLMENT OF THE REQUIREMENTS FOR
THE DEGREE OF MASTER OF SCIENCE IN HYDRAULIC ENGINEERING

MARCH, 2025

SCHOOL OF GRADUATE STUDIES

HAWASSA UNIVERSITY ADVISORS' APPROVAL SHEET

This is to certify that the thesis entitled "FLOOD HAZARD MODELING AND RISK MAPPING: CASE STUDY ON LOWER WEITO RIVER RIFT VALLEY BASIN SNNPR, ETHIOPIA..**"** submitted in partial fulfillment of the requirements for the degree of **Master's** with specialization in **Hydraulic Engineering,** the Graduate Program of the **Department of Hydraulic and Water Resource Engineering,** and has been carried out by **Gelma Boru** ID.No. **GPHydrR/0003/15**, under my supervision. Therefore i recommend that the student has fulfilled the requirements and hence hereby can submit the thesis to the department.

Dr. Abebe Tadesse (PhD)	_____	_____
Name of major advisor	Signature	Date

SCHOOL OF GRADUATE STUDIES

HAWASSA UNIVERSITY EXAMINERS' APPROVAL SHEET

We, the undersigned, members of the Board of Examiners of the final open defense by **Gelma Boru** have read and evaluated his thesis entitled "FLOOD HAZARD MODELING AND RISK MAPPING: CASE STUDY ON LOWER WEITO RIVER RIFT VALLEY BASIN SNNPR, ETHIOPIA**."**, and examined the candidate. This is, therefore, to certify that the thesis has been accepted in partial fulfillment of the requirements for the degree of Master of Science.

Dr. Abebe Tadesse (PhD)	_____	_____
Name of Major Advisor	Signature	Date
_____	_____	_____
Name of Internal Examiner	Signature	Date
_____	_____	_____
Name of Chairperson	Signature	Date
_____	_____	_____
Name of External examiner	Signature	Date
_____	_____	_____
SGS Approval	Signature	Date

DECLARATION

I hereby declare that this research work titled "**Flood hazard modeling and risk mapping: case study on Lower Weito River Rift Valley Basin SNNPR, Ethiopia.**" is my original work and has not been presented for a degree in any other university, and all sources of material used for this dissertation have been duly acknowledged.

Name: _____

Signature: _____

Date: _____

LIST OF ABBREVIATIONS AND ACRONYMS

1D	1 dimensional
2D	2 dimensional
Arc GIS	Aeronautical Reconnaissance Coverage Geographic Information System
DEM	Digital Elevation Model
DPPA	Disaster Prevention and Preparedness Agency
DTM	Digital Terrain Model
EPoA	Emergency Plan of Action
EV1	Extreme Value Type I
EV2	Extreme Value Type II
EV3	Extreme Value Type III
FEMA	Federal Emergency Management Agency
FLO-2D	Two-dimensional flood routing model
HEC-DSS	Hydrologic Engineers Center - Data storage system
HEC-RAS	Hydrologic Engineers Center - River Analysis system
ISDR	International Strategy for Disaster Reduction
TIN	Triangular Irregular Network
TUFLOW	Two-dimensional Unsteady Flow
USACE	United States Army Corps of Engineers
USGS	United States Geological Survey

TABLE OF CONTENTS

LIST OF FIGURES

LIST OF TABLES

DECLARATION

I, hereby declare that this M.Sc. thesis is my original work and that has not been presented for a degree in any other university and all sources of material used for this thesis proposal have been duly acknowledged.

Name: Gelma Boru

Signature: _____

Date: _____

ACKNOWLEDGMENTS

First of all, I would like to thank the almighty God for his endless and invaluable help to be a person of this stage and being able to complete this Master's program. Next, my deepest appreciation and respect full thanks will go to my advisor **Dr. Abebe Tadesse**, for his constructive guidance, innovative suggestions, and the leading role which contributed to the successes of this thesis research.

I would like to appreciate the Ministry of Water, Irrigation, and Energy particularly Hydrology and GIS department and that provided me with the data and information needed for this work.

ABSTRACT

*This study focuses on the modeling and mapping of flood inundation and associated risks in the Lower Weito River, a tributary of Lake Abaya by means of coupled hydrological and hydraulic models with different return periods. Meteorological, hydrologic, and topographic data were collected from various sources. Rainfall data from 1990 to 2015 were collected from the National Meteorological Agency and the stream flow data from 1990 to 2007 were collected from the Ministry of Water and Energy. DEM 12 * 12m resolution was downloaded from Alaska satellite facility, soil data was taken from FAO and LULC data were collected from the Ministry of Water and Energy. These data were integrated using modeling tools such as HEC-HMS and HEC-RAS, along with GIS software. To examine the accuracy of the HEC-HMS model, calibration and validation is performed using observed stream flow data. The results showed a strong relationship between simulated and observed data, with R2 and NSE values of 0.82 and 0.77, for calibration periods and 0.78 and 0.75 for validation period respectively which indicating a very good agreement between observed and simulated flow . The calibrated and validated model was then used to develop flood hydrographs for different return periods based on frequency storm analysis. The result of flood frequency analysis showed minimum peak flow of 77.9m^3/s for a 2-year return period with 24-hour storm duration and, the maximum peak flow 606.2 m^3/s occurs with a 100-year frequency storm for the same duration. The HEC-RAS model was used to generate flood inundation maps, which revealed the extent of flooded areas and the maximum flood depths and velocities for various return periods. The results indicated that the areas inundated by floods ranged from 1711.2 hectares for a 10-year return period to 2763.3 hectares for a 100-year return period. The maximum flood depths varied from 5.2 meters for a 10-year return period to 7.5 meters for a 100-year return period. The maximum flood velocities ranged from 3.15 meters per second for a 10-year return period to 7.01 meters per second for a 100-year return period. Flood hazard maps were derived by considering the depth, velocity, and duration of floodwaters. The results showed that about 0.01% of the total flooded area was under extreme hazard, 14% under very high hazard, 29% under high hazard, 35% under medium hazard, and 21% under low hazard. The flood vulnerability map classified the flooded areas into five vulnerability classes. Approximately 44% of the flooded area was classified as high and very high vulnerability, 19% as moderate vulnerability, and 37% as low or very low vulnerability. The flood risk map was developed by combining the flood hazard and vulnerability information. The results showed that 16% of the area was classified as very high to high risk, 46% as medium risk, and 38% from low to very low risk.*

Keywords: Weito River, Flood Vulnerability, Flood Risk; HEC-HMS, HEC-RAS

1. INTRODUCTION

1.1. Background

Floods can be explained as excess flows exceeding the transporting capacity of river channel, lakes, ponds, reservoirs, drainage system, dam and any other water bodies, whereby water inundates outside water bodies areas. Floods are natural phenomena that occur when streams, rivers, and lakes overflow their banks (Awal & Shakya, 2007). In the context of natural disasters, floods defined by the amount of damage they cause to people or property. If people did not inhabit flood-prone areas, the natural phenomena of a river exceeding its notional capacity and overflowing into the surrounding areas lead a natural disaster, property damage of any country (Awal & Shakya, 2007). Flood is one of the major natural disasters that have been affecting many countries or regions in the world year after year. An inundation map displays the spatial extent of probable flooding for different scenarios and can be present either in quantitative or qualitative ways.

Hazard is a potentially damaging physical event, phenomenon that may cause the loss of life or injury, property damage, environmental degradation, social and economic disruption. Hazards can include latent conditions that may represent future threats and can have different origins: natural (geological, hydro meteorological and biological) or induced by human processes (environmental degradation and technological hazards) (Awal & Shakya, 2007).

The goal of flood hazard assessment is to understand the probability that a flood of a particular intensity will occur over an extended period. Hazard assessment aims to estimate this probability over periods of years to decades to support risk management activities. Intensity usually refers to the combination of flood depth and horizontal flood extent; although other intensity measures such as flow, velocity and flood duration can also be important depending on the situation.

The other major component of flood risk, aside from flood hazard, is flood vulnerability. The goal of vulnerability assessment is to understand how a system will affect by floods. Examples of possible systems could include physical structures such as houses or bridges that could damage or destroyed a business or service whose supply chain could face interruption, or a community that could suffer fatalities, property losses, and negative health impacts in the aftermath of a flood. An important consequence of flooding is the

damage to physical structures such as buildings, bridges, roads, and public utilities. Damage can be defined as the amount of money needed to restore the area back to its original condition before the disaster and can be caused by lateral pressure forces, velocity forces, uplift, erosion of foundations, gradual weakening due to water logging, and other effects. Several factors are there that contribute to the flooding problem ranging from topography, geomorphology, engineering structures failures, climate, poor drainage and other local factors can be mentioned. Factors need to be considered in accurate flood hazard mapping under conditions of data and other material scarcity that notify the situation in most studies in Ethiopian. For instance, flood-generating parameters such as topography, soil, land use /cover, rainfall and stream flow collected from GIS (Geographic Information System) department, Ministry of water and Energy Authorities, Ethiopian and National Metrological Agency.

The problem of river flooding due to excess rainfall in short time and the following high river discharge is a great concern in the Weito River lake Basin of Ethiopia. In the main rainy season (March, April, and May); the floodplain of the River extends to particular areas not normally covered with water. In this basin, the river flooding usually occurs in the low-lying flat topographic areas of South Omo zone Bena Tsemay and Hamer woredas and in konso zone kolime woreda.

1.2. Statement Problem

Flooding is a continuous and recurring natural event in Ethiopia, particularly in floodplains where over 80% of annual precipitation occurs during the four wet months of June, July, August, and September Gebre (2015). The problem is exacerbated in highland areas due to significant environmental degradation driven by population pressures and the national topography, which consists of highland mountains and lowland plains with natural drainage systems, formed by the principal river basins. Historically, Ethiopia has faced severe flooding during its main rainy season, marked by unprecedented events of considerable magnitude and damage Khattak et al., (2016). These flood disasters result from the interaction of natural phenomena with environmental, social, and economic processes. Therefore, an integrated approach to flood assessment is essential, one that encompasses an understanding of both social and physical vulnerabilities to flooding hazards, as well as knowledge of the geomorphic and hydrologic characteristics of flood risks and the societal perceptions surrounding those Vojtek & Vojtekov, (2016). The

Weito River, which rises from the Guge Mountains and flows south into Lake Chew Bahir, delineates the boundary between Hamer Bena woreda and the Konso zone, as well as part of the boundary between the Southern Nations, Nationalities, and Peoples Region and the Oromia Region. This river conveys substantial runoff from upper catchments and local rainfall on the floodplain, leading to significant flooding problems. The diverse topography of the area, ranging from very flat to dissected plateaus, contributes to heavy flooding in low-lying regions, particularly in the Weito River Sub-basin of Bena Tsemay woreda, Hamer woredas, and Konso zone Kolime woreda. Flooding occurs when the volume of water in a river or stream exceeds the channel's capacity. The very flat lands, especially the floodplains in South Omo Zone, Bena Tsemay, Hamer woredas, and Konso zone Kolime woreda, are particularly susceptible to annual flooding during the rainy season. This ongoing issue has raised concerns among local communities, who rely on their social networks as floods become increasingly frequent.

During periods of high rainfall, the overflow of the river causes a series of flood hazards and risks. Many community members reside along the riverbanks to utilize water for agro-economic development, specifically through crop production supported by localized irrigation systems. However, due to the essential requirements of human life, they are compelled to live near the river, making them vulnerable to the unexpected occurrence of flooding, which damages their property each year. This study focuses on the flood problems affecting the South Omo Zone, particularly in Bena Tsemay and Hamer woredas, and Konso zone Kolime woreda, along the downstream area of the Weito River in Ethiopia

1.3. Objective

1.3.1. General Objective

The general objective of the study was to model flood hazard and risk map of the Lower Weito River RVLB, Ethiopia.

1.3.2. Specific Objectives

The specific objectives of the study were:

- To estimate peak flood discharge for different return periods
- To develop the flood inundation map of the study area

- To develop the flood hazard map for the affected areas in the Lower Weito River
- To develop a flood risk map for a vulnerable area

1.4.Research Questions

- How much is the peak flood discharge for various return periods?
- How big is the inundated flood area due to the various return period flood magnitudes?
- How to develop a flood hazard and vulnerability map of the study area?
- How to develop a potential flood risk map?

1.5.Scope of the Study

The study aimed at of flood hazard and risk modeling of the Lower Weito catchment Rift Valley Lakes Basin. In this study the inflow runoff hydrograph for different return periods will be determined using rainfall-runoff hydrological model, inundation and risk mapping will be prepared using hydraulic model and Arc GIS and appropriate mitigation flood measures will be proposed.

1.6. Significance of the Study

The significance of this study was to update and expand information on stream flow, and river characteristics crossing rural settlements town and provide an updated flood map to water resource managing and planning sector. These help them to have good information about integrated land use planning and manage for flood plain area. In addition to this, the outcome of this study will give the updated information for the downstream dwellers on the effect of peak discharge from the Lower Weito River. The well-informed population of upstream catchment characteristics will be aware of unexpected flooding in the future.

1.7. Thesis organization

Generally, the thesis was structured into five chapters, a reference list, and appendices. Chapter One introduces the study with its objective, statement of the problem, Scope, and significance of the study. Chapter two describes the literature review related to the study. Chapter three deals with the materials and methods that are used in the study. In this chapter, the study area was described, the available data were collected and analyzed and the procedures to address the study objective were well defined. Chapter four describes the results and discussions and chapter five deals with conclusions and recommendations of the study. The reference list outlines the bibliography of the materials to which the

respective citations refer. The Appendix provides supplementary information on the materials used and the results of the study.

2. LITERATURE REVIEW

2.1. Flooding

Flooding is the most common natural disaster around the world in terms of life loss and damage to properties and infrastructures Javadnejad et al., (2017). Dilley et al., (2005) estimated that more than one-third of the world's land area is flood-prone affecting 35 percent of the world's population. During the past 20 years, worldwide natural disasters have resulted in the death of at least 3 million people, while also adversely affecting nearly 800 million people. It has been determined that 30 out of 40 natural disasters occur in Iran, where flooding has been highlighted as the most damaging one Safaripour et al., (2012).

In the world, 2.3 billion people were affected by floods between 1995-2015 Serra-Llobet et al., (2018).

In Africa, floods of different kinds are one of the most common types of disastrous events, and they account for the biggest losses inflicted by natural disasters. The UN Office for the Coordination of Humanitarian Affairs (OCHA) recently stated that, compared with previous years, 2010 has seen the largest number of people affected and dying from flooding. This is consistent with the dramatic rise in flood events that have battered the world, with West Africa being a case in point S. I. Khan et al., (2011)

According to the Ethiopian Government Disaster Prevention and Preparedness Agency (*Ethiopia*, 2006), the leading government agency in disaster management, more than 500,000 people are vulnerable, and more than 200,000 people have been affected, with 639 people deaths (364 people in South Omo, 256 people in Dire Dawa, and 19 people in other parts of the country). Thousands of livestock will be killed, 228 tons of harvest was held away, 147 tons of export coffee beans will be lost (and machinery ruined), and 42,229 hectares of crops will be inundated.

In Ethiopia, rainfall attributed to the Kiremt rains, which began on 8 June to 15 August has led to extensive flooding. The Ambeira zone in Afar region, and special zones surrounding Addis Ababa (the capital), Jima, South-east Shewa, and South-west Shewa in the Oromia region have been worst affected by the rains and flooding. It is estimated that a total of 18,628 households (HHs) (93,140 people) have been affected, of which 7,270 HHs (36,350 people) have been displaced (*Ethiopia*, 2020).

2.2. Flood Frequency Analysis

According to Khadka (2014), hydrologic systems are sometimes impacted by extreme events, such as severe storms, floods, and droughts. The magnitude of an extreme event is inversely related to its frequency of occurrence, with very severe events occurring less frequently than more events that are moderate. Estimating flood magnitudes and their frequencies requires knowledge related to distributions of flood flow series. Probability for future events can be predicted by fitting past observations to selected probability distributions. The primary objective is to relate the magnitude of these extreme events to their frequency of occurrence through the use of probability distributions (Khadka, 2014). In this case, flood frequency analysis is the most suitable method to determine a robust probability distribution that fits to stream flow data at a certain location of interest. The most widely used methods in predicting flood magnitudes are at-site and regional flood frequency analyses Zakaria & Shabri, (2012). When the stream flow is selected for flood frequency analysis, there are two methods of compiling flood peak data, annual maximum and partial duration serious. Annual maximum serious takes the single maximum peak discharge in each year of record so that the number of data values equals the record length in years whereas partial duration takes all the peak over a selected level of discharge, a threshold Adeyi et al., (2020). However, the partial duration is limited by the fact the observation may be dependent which violates the assumption of independence of flood peak for statistical analysis A.O. & Njogu, (2020).

2.3.Probability Distributions of Hydrologic Variables

According to Khadka (2014), there are several distributions in hydrology used to analyze the probability of occurrence of a stream flow.

2.3.1. Log-Pearson type III distribution

The Log-Person Type III distribution is a member of the family of Pearson III distribution, and is also referred to as the Gamma distribution. Log-Person Type III distribution is derived by change of variable on the logarithms of this variable. This is the current required method to be used for frequency analysis in the United State. The location of the bound ϵ in the log-Pearson Type III distribution depends on the skewness of the data. If the data are positively skewed, and then $\log X \geq \epsilon$ and ϵ is a lower bound, while if the data are negatively skewed, $\log X \leq \epsilon$ and ϵ is an upper bound. The log

transformation reduces the skewness of the transformed data and may produce transformed data that are negatively skewed from original data that are positively skewed. In that case, the application of the log- Pearson Type III, raises a problem that is the tendency to give low upper bounds on the magnitude of the data A.O. & Njogu, (2020).

2.3.2. Extreme value distribution

The General Extreme Value is the family of a continuous probability distribution that combines the Gumbel (EV1), Weibull (EV2), and Frechet distribution (EV3). GEV makes use of three parameters; location, scale, and shape. The location parameter describes the shift of distribution in a given direction on the horizontal axis. The scale parameters describe how spread out the distribution is and define where the bulk of the distribution lies, as the scale parameter increases, the distribution will become spread out. The third parameter in the GEV family is the shape parameter which strictly affects the shape of the distribution and governs the tail of each distribution. The shape parameter is derived from Skewness, as it represents where the majority of the data lies. This creates the tail of the distribution when shape parameter (K) = 0, this is the EV1distribution, for which the EV2 is when K> 0, and for K<0 the distribution is EV3. The Gumbel (EV1) and Weibull (EV2) distributions are used for extreme (maxima and minima values) respectively of hydrological variables. The EV1 distribution is used in the frequency analysis of floods and the EV2 distribution in the analysis of low flow values observed in a river A.O. & Njogu, (2020). Gumbel extreme value distribution aims to build the relationship between the probability of the occurrence of a certain event, its return period, and its magnitude El-Naqa & Zeid, (1993).

2.3.3. Exponential distribution

Some sequences of hydrologic events, such as the occurrence of precipitation, may be considered Poisson processes, in which events occur instantaneously and independently on a time horizon, or along a line. The time between such events, or inter-arrival time, is described by the exponential distribution whose parameter λ is the mean rate of occurrence of the events. The exponential distribution is used to describe the inter arrival times of random shocks to hydrologic systems, such as slugs of polluted runoff entering streams as rainfall will beeches the pollutants off the land surface. The advantage of the exponential distribution is that it is easy to estimate $\boldsymbol{\lambda}$ from observed data and the exponential distribution lends itself well to theoretical studies, such as a probability model for the linear reservoir ($\boldsymbol{\lambda}$ = l/k, where k is the storage constant in the linear

reservoir). Its disadvantage is that it requires the occurrence of each event to be completely independent of its neighbors, which may not be a valid assumption for the process under study for example, the arrival of a front may generate many showers of rain and this has led investigators to study various forms of compound Poisson processes, in which λ is considered a random variable instead of a constant Govindaraju & Levent, (1993).

2.3.4. Gamma distribution

The time taken for the number ß of events to occur in a Poisson process is described by the gamma distribution, which is the distribution of a sum of ß independent and identical exponentially, distributed random variables. The gamma distribution has a smoothly varying form like the typical probability density function and is useful for describing skewed hydrologic variables without the need for log transformation. It has been applied to describe the distribution of depth of precipitation in storms.

According to Adeboye & Alatise, (2007), the two-parameter gamma distribution (parameters ß and υ) has a lower bound at zero, which is a disadvantage for application to hydrologic variables that have a lower bound larger than zero.

In determining correct distributions, the concern is to find the one that would be capable of describing the recorded sample and more importantly, extrapolating correctly to large return periods. Many distribution function forms have been proposed for describing flood occurrences. However, previous studies have reported in their literature that there is no „universal" distribution function that represents flood trends at all steam flow locations of interest Zakaria & Shabri (2012)

2.3.5. Normal distribution

The normal distribution is used in frequency analysis for fitting empirical distributions to hydrological data and in the simulation of data. As many statistical parameters are approximately normally distributed, the normal distribution is often used for statistical inferences. An early application of the normal distribution to hydrologic variables will be by Adeboye & Alatise (2007), who introduced the normal probability paper for analysis of hydrologic data. Phien, (2001) found that the normal distribution could be used to fit the distribution of annual rainfall and runoff data. Haghighat, (2016) demonstrated that, in the absence of information about the distribution of floods and economic losses associated with the design of flood reduction measures, the use of the normal distribution is better than other distributions such as extreme value, log-normal or Weibull.

2.3.6. Three-Parameter Log-normal (LN (3P)) Distribution

The Log-normal (3p) distribution is a member of the family of Normal distribution. It is the most widely used distribution function for the determination of flood. It is also a standard method to compute peak floods in the United States Busby, (2017).

According to Demissie (2008), in large-scale studies, many countries adopted standard methods that can be used by scholars or agencies to produce uniformity in conducting flood frequency analysis. For instance, the United States Water Resource Council recommends the three-parameter lognormal distribution where in a similar study. The United Kingdom and Ireland proposed the GEV distribution as a standard. The Person III and Log Person III distribution were generally recommended in Germany.

2.4. Software used for the study

2.4.1. Geographic Information System

Geographic information system (GIS) is a tool that can be used in every step of flood risk assessments for visualization, data management, and modeling Yusoff et al., (2008).

According to Khaligni, (2015), GIS is a system for capturing, storing, checking, identifying, manipulating analysis, and displaying data, that are spatially referenced to the earth. Using GIS to a large extent facilitates providing accurate information as it can handle the digital data along with their associated attribute information on physical and environmental aspects. The capability of applying GIS to the flood simulation assists in analyzing the flood level or extent spatially. It helps in visualizing flood simulation in an interactive setting, where the spatial impact of various scenarios can be viewed along with the location of critical facilities and thus assess the vulnerability of the region towards a flood event efficiently Yerramilli, (2012).

2.5. Hydrological Models

Hydrological models are a simplified, conceptual representation of the components of the hydrologic cycle. There are different forms of hydrological models and are primarily developed for a better understanding of the hydrologic processes and prediction of hydrologic phenomena in a watershed.

2.5.1. Types of hydrological models

According to Chow, (1988), stochastic and deterministic models are often considered to be at the top level of the classification tree, under the way they treat the randomness of hydrologic phenomena. Stochastic models use local hydrometric data to predict flows.

These models allow for some randomness that results in different outputs based on analysis of past events, commonly rainfall and river discharge Ahmad et al., (2001). Deterministic models generally produce a single output of runoff for a given rainfall under identical physical environments. Without going into too much detail, deterministic hydrologic models can be classified into three main categories (Cunderlik, 2003).

Lumped models: lumped hydrologic model simulation evaluated only at the outlet of the basin that is without explicitly accounting for the response of individual sub-basins and parameters do not vary spatially within the basin. Parameters of lumped models often do not represent the physical features of hydrologic processes and usually involve a certain degree of empiricism. According to Haan et al. (1994), the impact of spatial variability of model parameters is evaluated by using certain procedures for calculating effective values for the entire basin and the most commonly employed procedure is an area-weighted average. Lumped models are not usually applicable to event scale processes. If the interest is primarily in the discharge prediction only, then these models can provide just as good simulations as complex physically based models (Beven K. , 2000). The water balance model (WATBA), Snowmelt Runoff Model (SRM), Identification of unit Hydrograph and Components from Rainfall, Evaporation, and Stream flow data (IHACRES) are examples of lumped hydrological models

Distributed models: distributed hydrological model parameters are fully allowed to vary in space at a resolution usually chosen by the user. The distributed modeling approach attempts to incorporate data concerning the spatial variation of parameters together with computational algorithms to evaluate the influence of this distribution on simulated precipitation-runoff behavior. Distributed models require large amounts of data for parameterization in each grid cell (Beven, 2006). However, the governing physical processes are modeled in detail, and if properly applied, they can provide the highest degree of accuracy. For instance, HYDROTEL, MIKE11/SHE and WATFLOOD are distributed models.

Semi-distributed models: parameters of semi-distributed models are partially allowed to vary in space by dividing the basin into several smaller sub-basins. Semi-distributed model structures are more physically based than the structure of lumped models and have less demanding input data than fully distributed models. Semi-distributed models can be grouped with Kinematic Wave theory models and probability-distributed models.

According to Beven (2000), the Wave theory models are simplified versions of surface and/or the subsurface flow equations of physically based hydrologic models. In the case of the probability-distributed models, spatial resolution is considered by using probability distributions of input parameters across the basin. Examples of semi-distributed models are SWAT (Arnold et al., 1993), HEC-HMS (US-ACE, 2001), HBV (Bergström, 1995), and TOPMODEL (Cunderllk, 2003).

2.6.Model Selection

Selecting the best and appropriate model is an essential part of any research work. There are various criteria for choosing the most suitable model. According to Cunderllk & Simonov, (2007), the choice depends mainly on the requirements and needs of the research under interest. Cunderllk & Simonov (2007) will put the following as criteria: the required output of the model, Availability of input data, Prices and availability of the model, and the model structure. Some of the factors and criteria involved in the selection of a model for this study include free, simple to use, the importance of the required model output, availability and quality of data, the hydraulic and hydrogeological characteristics of the basin, the availability and size of computers for model development and operation. 2D Flood Modeling is selected due to no need to predefine the flow routes, Easy to setup, can be more accurate, Velocity variation on flood plains, Flood maps, and depth grids at direct output. In this research, the 2D hydraulic model (HEC-RAS) with ArcGIS was used for hydraulic modeling whereas the choice of a suitable hydrological model depends on the function that the model needs to serve and several hydrological models simulating the hydrological process at different spatial and temporal scales. For this study, the HEC-HMS model was selected since it fulfills the above criteria. Besides, the model was selected because, it is physically based, semi-distributed belongs to the public domain, and is computationally efficient in simulating the hydrological characteristics of the watershed.

2.6.1. Hydrologic modeling (HEC-HMS)

HEC-HMS (the Hydrologic Engineering Center's Hydrological Modeling System) Model developed by the US Army Corps of Engineers is designed to simulate the precipitation-runoff processes of dendritic watershed systems (USACE, 2005). HEC-HMS conceptually represents watershed behavior as different components of runoff processes. It has an appropriate representation of the hydrological system, and its specification depends upon the information needs of the hydrological study. Hydraulic

modeling and inundation mapping, the main objective is to accurately predict catchment outflows from upstream sub-catchments and flood wave propagation along the drainage network. A model relates something unknown (the output) to something known (the input). In the case of models included in HEC-HMS, the known input is precipitation and the unknown output is runoff, or the known input is the upstream flow and the unknown output is the downstream flow (*USACE*, 2005).

HEC-HMS consists of separate models of the major hydrological processes and transports. It consists of runoff volume models, models of direct runoff (overland flow and interflow), base flow models, and channel flow models. HEC-HMS gives flexibility to the user by providing each component with a suit of models. The user chooses a suitable combination of models depending on the availability of data, the purpose of modeling, and the required spatial and temporal scale (Asadi, 2013).

HEC-HMS computes runoff volume by computing the volume of water that is intercepted infiltrated, stored, evaporated, or transpired and subtracting it from the precipitation. Interception, infiltration, storage, evaporation, and transpiration collectively are referred to in the HEC-HMS program and documentation as losses (Feldman, 2000).

2.6.2. Hydraulic Modeling (HEC-RAS)

Hydrodynamic models are Numerical flood models or computer-based models that use mathematical and computational techniques to simulate the behavior of water during a flood event (Anees et al., 2016). These models typically employ numerical algorithms to solve equations that describe the flow of water in a river or stream, while taking into consideration factors such as rainfall, runoff, channel geometry, and riverbed roughness. Numerical flood models can be used to simulate the effects of various flood scenarios, as well as to assess the efficiency of the proposed flood mitigation measures (Saleh et al., 2013). They are also used to simulate how flood behavior will alter in response to changes in climate, land use, and other factors. Numerical flood models can take several forms, such as one-dimensional models that simulate water flow in a river channel (Pramanik et al., 2010) or two-dimensional models that simulate water flow over a floodplain (Rameshwaran & Shiono, 2007).

Hydrodynamic models are widely used tools in detailed flood dynamics simulations and are mostly linked to flood forecasting, and mapping (Anees et al., 2016). The critical characteristics of hydrodynamic models that perhaps explain their widespread usage in

various applications are the ability to manipulate their inputs to investigate the impacts of changes in the initial conditions, boundary conditions, and topographic changes arising from the change in critical hydrodynamic features such as river streams, culverts, and stream channel volume (Randa et al., 2022). The 1D hydrodynamics are usually computationally efficient since they consider flows in one direction and assume their steady and uniform. However, they have several limitations which include the inability to capture lateral and vertical wave diffusions of the flood waves, considering topography as cross-sections rather than the continuous surface, and thus somehow subjective in factoring in orientation and topographical cross-sections (Horritt & Bates, 2002). The 2D hydrodynamics generally can accurately simulate inundation timings and durations and are thus commonly used in different applications. However, they are computationally intensive especially when covering a large study area since they solve the full shallow-water equation (Neelz & Pender, 2010). The 3D hydrodynamic models are generally considered not viable when covering an area of more than 1000 square Kilometers especially when a high-resolution simulation is required. They are computationally intensive and may take prohibitively long and thus not reliable for quick forecasts that give enough lead time for interventions (Beven & Binley, 1992). For numerical flood modeling, several packages are available, including:

- HEC-RAS: This software, created by the US Army Corps of Engineers, is used to simulate the hydraulics of river systems in both one and two dimensions (Khattak et al., 2016);
- MIKE FLOOD: This software, which was created by DHI, is utilized for the two- and three-dimensional hydraulic modeling of floodplain and river systems (Tansar et al., 2020);
- TUFLOW: This software is used for the two-dimensional and three-dimensional hydraulic modeling of floodplain and river systems (Fahad et al., 2020);
- Flood Estimation Handbook (FEH) models: Developed by the United Kingdom Environment Agency, used for rainfall-runoff modeling and flood frequency analysis (Faulkner & Wass, 2005);
- Environmental Protection Agency's Environmental Fluid Dynamics Code (EFDC): This software, developed by the United States Environmental Protection Agency, is used for three-dimensional hydraulic and water quality modeling of surface water systems (Roy et al., 2020).

Benefits of 2D models

Fewer modeling assumptions and less user judgment yield results that are representative of actual conditions. Enhanced communication with stakeholders with engaging graphics, videos of flow paths, and georeferenced results.

Accurate representation for complex conditions, including wide floodplains, sinuous channels, multiple channels, bends and confluences, bridge/roadway crossings, roadway overtopping, skewed roadway, tidal waterways, and bridge scour, among other conditions.

2.7.Flood Inundation Mapping

Flood inundation maps indicate flooded areas that are affected by or vulnerable to a particular hazard. Flood inundation maps were generated using ArcGIS (Kumar et al., 2017). It helps to prevent serious damage and deaths. It is a vital component for appropriate land use planning in flood-prone areas. It creates easily-read, rapidly-accessible charts and maps which facilitate the administrators and planners to identify areas of risk and prioritize their mitigation/response efforts as nonstructural measures (Pasche, 2008).

An inundation map displays the spatial extent of probable flooding for different scenarios and can be presented either in quantitative or qualitative ways. The inundation or hazard assessment mapping delineates flood hazard areas in the river basin by integrating local knowledge, and hydrological, meteorological, and geomorphologic data using different approaches. The inundation is an essential component of emergency action plans; it supports policy and decision-makers in deciding how to allocate resources, flood forecasting, and significant land use planning in flood-prone areas (Gebre Sl, 2015).

Inundation maps can have different uses including emergency action plans, mitigation planning, emergency response, and consequence assessment (FEMA, 2013).

1. Emergency action plans (EAP): An Emergency Action Plan is used to identify potential emergency conditions at a dam and specifies preplanned actions to minimize property damage and loss of life. The downstream inundation map is the basis for developing the Emergency Action Plan and is used to show the emergency management authorities and the critical areas for action in case of an emergency.

2. Emergency response: Emergency response represents the actions taken in the aftermath of an incident to save and sustain lives, meet basic human needs, and reduce the loss of

property and the effect on critical infrastructure and the environment. In the case of dam failures and incidents, this would be the response by the dam owner, and local community emergency management to minimize the consequence of actual dam failure or incident.

3. Hazard mitigation planning: Mitigation is the proactive effort to reduce loss of life and property by understanding the effects of disasters. This is achieved through identifying hazard potentials and the risks they pose in a given area. In the case of river flooding, hazard mitigation planning involves identifying the population at risk and identifying the action to reduce their vulnerability. Information required by hazard mitigation planners includes the inundation zone boundary, depth of flooding, velocity, and timing.

According to Nquot & Kulatunga (2014), flood risk management plans are based on five major elements: prevention, protection, preparedness, emergency response, and recovery. It is important to note that the preparation of flood risk maps and risk management plans do not by themselves stop the occurrence of floods. Therefore, appropriate mitigation measures should be taken in flood-prone areas. The question may arise to construct flood protection structures: how are these new structures to be built where would they be located; and of what materials are they to be built Nquot & Kulatunga (2014) argues for the need for economic, social, and environmental sustainability and the use of adaptive measures for new developments.

4. Flood consequence assessment: This includes identifying and quantifying the potential consequence of flooding or incident. While hazard mitigation planning focuses on the economic and social impacts of a potential disaster and the organizational and government action needed in the result of flooding to respond and recover.

2.7.1. Flood Inundation Map Elements

FEMA (2013) recommends that map collar information, base map data, inundation polygons, and Inundation elevation as elements of flood inundation maps.

1. Map collar information: The latitude and longitude coordinates are can be referenced at the corners of the neat line. The other important information displayed on the map collar can be horizontal reference grid ticks to help orient map users to real world coordinates.

2. Base map data: Base map data provide the background from which inundation hazard information is overlaid and interpreted. Clear, easy to interpret base maps are critical for the effective use of an inundation map.

3. Inundation polygons: Inundation polygons are used to define the horizontal limits of the inundated area for one or more breach events. The inundation polygon shows the

intersection of the peak water surface elevations from the dam breach model with the ground elevation with the terrain surface.

4. Inundation elevation: Inundation elevation can be explained at key locations along the inundation polygon if desired and extracted directly from the flood model. Elevations are not always a critical element for an inundation map. Elevation may be important for flood warning if early warnings are possible.

For this study, Three-Parameter Log-normal (LN (3)) Distribution, ArcGIS10.3, and HEC-RA 5.0.5 2D modeling software are selected for catchment characteristic determination and delineation of flood mapping respectively to meet the simulation requirements set above using available DEM, topography, land use/land cover and hydrology data.

2.8. Flood Hazard Mapping

Floods create hazardous conditions to which humans are particularly vulnerable. Flood hazard is typically defined as a product of the velocity and depth of floodwaters (Ndue & Baylie, 2023). Fast-flowing shallow water or deep water (even when flowing slowly) can unbalance people and vehicles and sweep them away. Similarly, floodwater and debris can undermine structures or damage or destroy structural and non-structural elements of buildings and infrastructure and affect contents (Grande, 2016). Hazardous flood conditions can exist without a flood risk. If floodplains were unoccupied and unused, flooding would still be hazardous but would not create a risk to the community. It is the human interaction with flooding that creates risk. Exposure can lead to the potential loss of life, injury, failure of buildings and infrastructure, and economic loss in future floods (Vojtek & Vojtekov, 2016). The degree of hazard varies with the severity of flooding and with flood extent, time, and location.

2.9. Flood Vulnerability Mapping

Flood vulnerability is one of the significant components in risk management and flood damage assessment. Since vulnerability is found to be the main reason for disasters, it seems necessary to develop our perception of vulnerability (Nasiri et al., 2016a). Research with vulnerability subjects involves diverse descriptions for vulnerability; in the United Nations' description vulnerability is a degree of damage to certain objects at flood risk with a specified amount and present in a scale from 0 to 1 (no damage to full damage) (UNU-EHS, 2006). The International Panel on Climate Change (IPCC)

described the vulnerability as the incapability degree of managing climate change and sea-level rise impacts(IPPC, 1995). Flood vulnerability is one of the significant components in risk management and flood damage assessment (Nasiri et al., 2016b). There are several methods developed by Researchers to evaluate flood vulnerability. Nevertheless, flood threats is still very prevalent despite increased awareness about the vulnerability (Birkmann, 2007). This matter increases doubt about the effectiveness of vulnerability evaluation methods and their influence on flood mitigation and adaptation(S. Khan, 2012). Vulnerability measurement is a complex process because it is influenced by several environmental, economic, and social or even political elements on a local scale (Nasiri et al., 2016a). In other words, vulnerability is affected by numerous factors such as settlement conditions, infrastructure, authority's policy and capacities, social inequities, economic patterns, etc.(Miranda & Ferreira, 2019). So flood vulnerability varies for people in diverse circumstances (Pandey et al., 2010). Human systems are vulnerable to floods due to three vital aspects: Exposure, susceptibility, and resilience. Exposure refers to people and their surroundings and every element present in flood-prone areas being exposed to the flood impacts as a subject to potential losses(UNISDR, 2009). Susceptibility (Tan et al., 2012) states is people, environment, and infrastructure tend to be influenced by a hazard because of the fragility of the community or ecosystem, and (Al, 2004) defines resilience, coping, and adaptation ability of a system in addressing disaster stress. Instance the vulnerability of urban areas is a reflection of the exposure and susceptibility of the city to flood risk and the resilience of that region to cope and recover from the flood effects (Smit, 2006).

Generally, the vulnerability of a system against a certain hazard is not easily assessed. Three routes for the assessment can be distinguished such as economic, social, and cultural.

Thus, vulnerability assessment in flood-prone areas depends on the following factors (Tsakiris, 2007):

- The Exposure of the system (E).
- The initial coping capacity (resources availability) of the system (S).
- The magnitude and intensity of the hazardous event (Qmax).
- The social response of the system (early warnings, indigenous experience, public awareness, etc.) (SF).

- The fuzziness of the interrelated sides of vulnerability (coping capacity & exposure) (I).

2.10. Flood Risk Analysis

According to (EU, 2022) for flood management, "flood risk" is the likelihood of a flood event together with the actual damage to human health and life, the environment, and economic activity associated with that flood event. In this context, flood risk can be considered as the actual threat, in other words, the real source of flood hazard to the affected areas. The quantification of flood risk results either in monetary units or in loss of life units, if the losses are measurable, or in qualitative terms (e.g. allocation in classes) in the case of intangible damages (social, environmental, cultural) to the affected areas.

Risk refers to the product of hazard (the physical agent and its impact) and vulnerability (the susceptibility to damage or injury) (Alexander, 1997). Developing a flood risk model involves two steps: hazard assessment and vulnerability assessment. Hazard assessment deals with the characteristics of the event itself in terms of magnitude and frequency. While vulnerability assessment takes into account the effects of the event on the population, considering social, economic, and environmental aspects and impacts on transportation infrastructure (Adigrat et al., 2019).

3. MATERIALS AND METHODS

3.1. Description of the Study Area

3.1.1. Location

Weito watershed is located at the lower part of Ethiopian Rift Valley Lakes Basin, between 36º30’00’’ E – 38º0’00’’ E longitudes and 4º30’00’’N - 6º15’00’’N latitudes. It is one of the main rivers flowing to Chew Bahir. It originates from the Guge Mountains, flowing south into Lake Chew Bahir, which found in between the border of Ethiopia and Kenya. (Ayana, 2019). The river length from its source was estimated to be 198.6km and the total catchment area of the basin was 4514.7km^2.

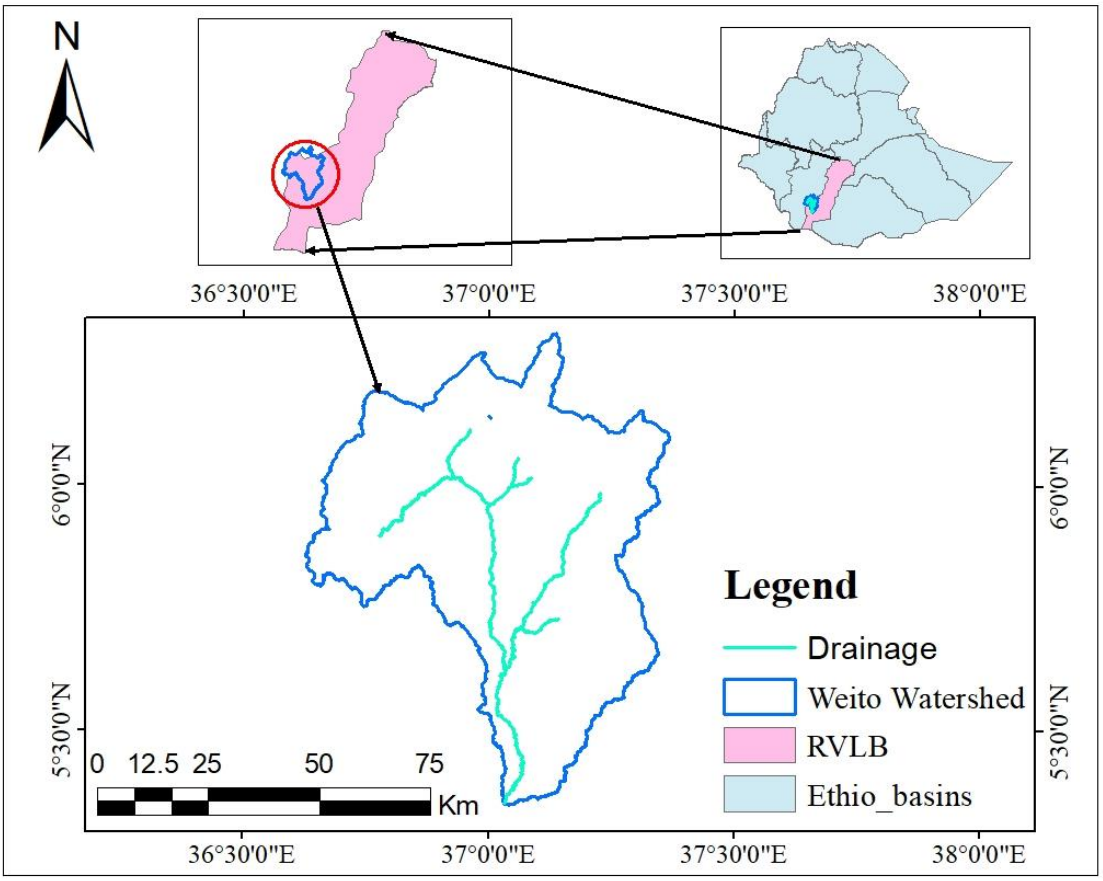

Figure 3.1: Location map of the study area

3.1.2. Topography

The basin's North West and North east are steep, while the lower areas are flat and have a vast valley. The elevation of an area ranges between 494m to 3414m.

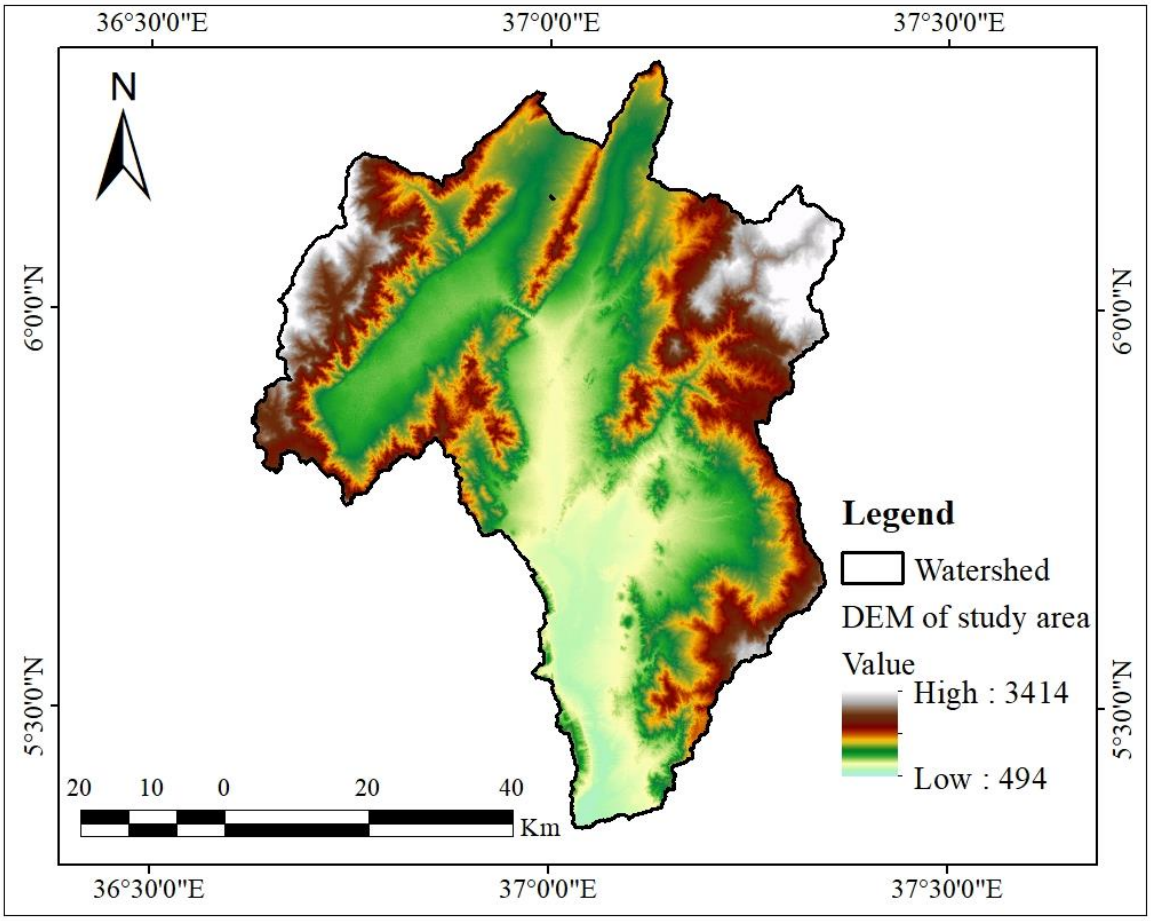

Figure 3.2: Topography of the study area

3.1.3. Soil

Soil in the study area is closely related to parent material and degree of weathering (Makin et al., 1976). Generally, major soil classes in Weito Watershed, are chromic Cambisols (loam to sandy loam), chromic Luvisols, chromic Vertisols, Dystric Cambisols, Eutric Cambisols, Eutric fluvisols, Eutric nitosols, and Orthic Acrisols.

.

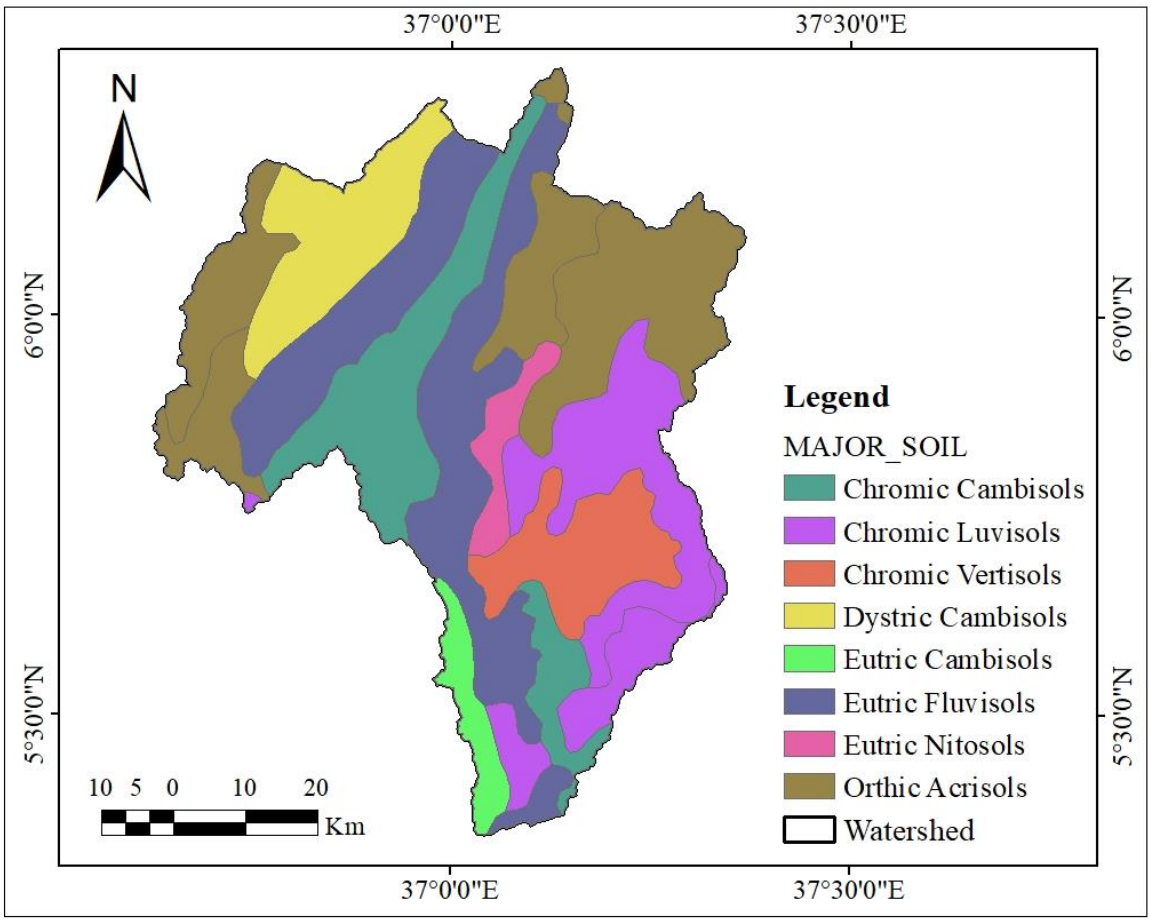

Figure 3.3: Soil Map of Weito watershed

3.1.4. Land use/Land cover

The catchment's land cover is influenced by topographical, climatic, and biological factors. The rift valley basin's land cover has changed dramatically in recent years as a result of population increase. The dominant land use land cover of Weito watershed was shown on figure below..

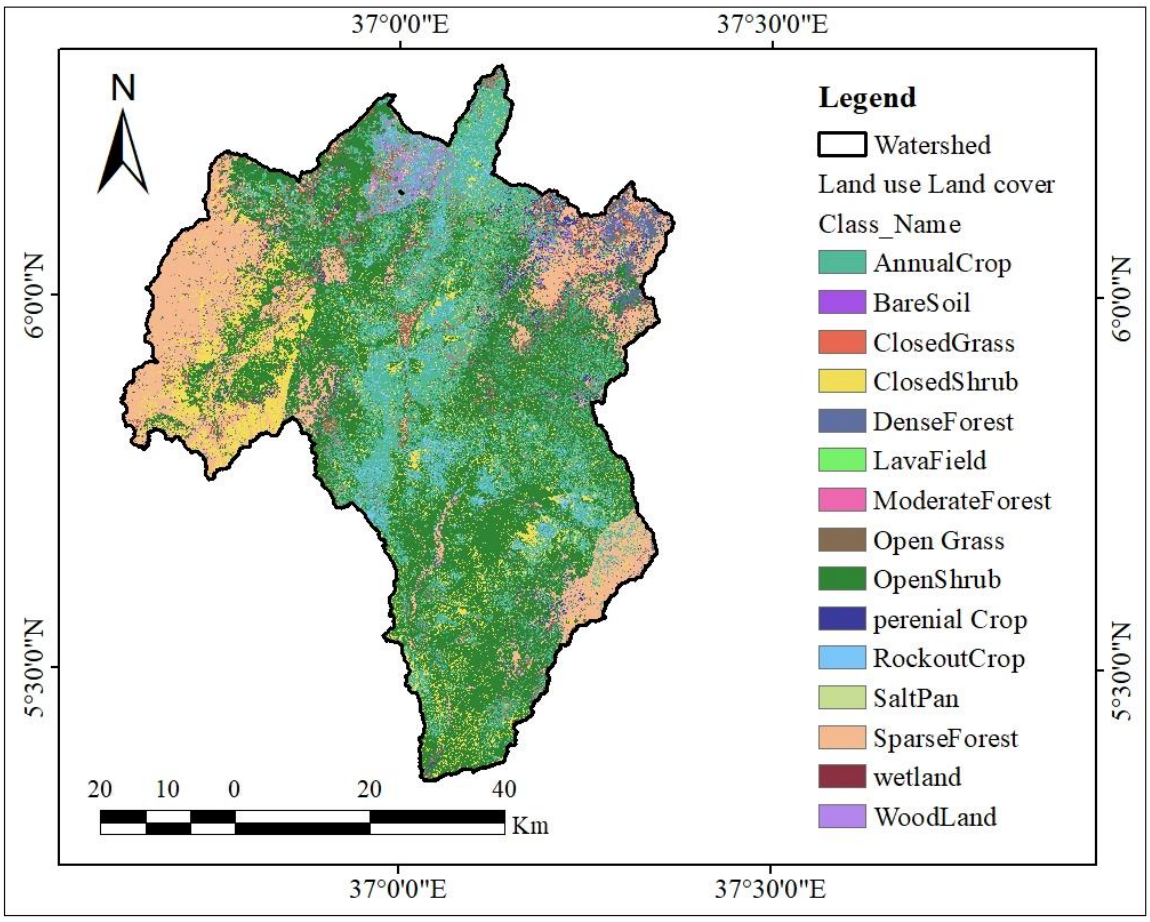

Figure 3.4: Land use Land cover Map of Weito watershed

3.2.Methods

3.2.1. Data collection

In order to achieve the objective of this study, different data was collected from different sources. These are hydro-meteorological data, DEM, soil, land use/land cover and socio-economic data. The stream flow data from 1990 to 2007 were collected from Ministry of Water and Energy, Ethiopia the rainfall data from 1990 to 2015 were collected from national meteorological Agency. The digital elevation model (DEM), data were downloaded from the Alaska satellite Facility, soil data from FAO websites and land use/land cover data from the Ministry of Water and Energy respectively. The manning's roughness coefficient were collected from field survey and verified with data from relevant literature (Chow, 1959).

3.2.2. Rainfall data

In this study, the rainfall data were collected from four meteorological stations (Beto-Ubadebretsehay, Benatsemay, Derashi and Konso-karate). The meteorological data was obtained from the National Meteorological Agency (NMA) and covered a period of 26 years from 1990 to 2015.

3.2.3. Stream flow data

The daily stream flow data collected from the Weito Bridge gauging station covered a period of 18 years (1990-2007). This data was crucial for model calibration, validation, and analyzing the impacts of meteorological factors on runoff generation and watershed response.

3.2.4. Digital Elevation Model (DEM)

Digital Elevation Model (DEM) is a square grid of regular spaced elevation data for hydrology, agricultural planning, soil mapping and so on. Unfortunately, the use of DEM surface is generally not suitable for large scale terrain representation for hydraulic analysis of the river channels. Because they cannot vary in the spatial resolution, it may poorly define the land surface in areas of complex relief. Therefore, for hydraulic modeling of river channels, the Digital Elevation Model (DEM) with spatial resolution 12.5m by 12.5 m were downloaded from the Alaska satellite Facility (https://vertex-retired.daac.asf.alaska.edu/).

3.3.Data Analysis

3.3.1. Tests on hydrologic data

The basic assumptions in statistical flood frequency analysis are the independence and stationarity of the data series and that the data come from the same distribution homogeneity and outlier, it is better to check the flow data at five percent significance levels to reach an accurate estimate.

3.3.1.1. Test of independence and stationarity

Wald-Wolfowitz (1943) (W-W) test were used to test for the independence of a dataset and to test for the existence of trends in a given sample of size N. For a dataset X1, X2.... Xn the statistic R was calculated.

$R = \sum_{i-1}^{N-1} X_i X_{i+1} + X_1 X_n$ ………………………………………………………………… (3.1)

Where: - X_i – Magnitude of flow at i period

X_{i+1} – Magnitude of flow next to i period

X_1 – Magnitude of flow at first period

X_n – Magnitude of flow at last period

N– Total number of flows

When the elements of the sample are independent, R follows a normal distribution with mean and variance given.

$$\bar{R} = \frac{S_1^2 - S_2}{N-1} \quad \ldots \quad (3.2)$$

$$Var(R) = \frac{S_1^2 - S_2}{N-1} - \bar{R}^2 + \frac{S_1^4 - 4S_1^2 S_2 + 4S_1^2 S_3 + S_2^2 - 2S_4}{(N-1)(N-2)} \quad \ldots \quad (3.3)$$

Where; $S_r = Nm'_r \ and \ m'_r = \frac{1}{n} \sum_{i-1}^{n} x_i^r$

$m'_r \ is \ the \ rth \ moment \ of \ the \ sample \ about \ the \ origin$

The statistic U is approximately normally distributed with mean zero and variance unity. In this thesis, the test of independence was at 5 % significance level, by comparing the statistic u with the standard normal variate $u_{a/2}$ corresponding to a probability of exceedance $a/_2$.

$$U = \frac{R - \bar{R}}{\sqrt{Var(R)}} \quad \ldots \quad (3.4)$$

3.3.1.2. Tests of homogeneity and stationarity

The Mann- (Whitney, 1947) test considers the quantities V and W by testing two samples of size p and q, where p is less than or equal to q are compared. The combined data set of size N = p + q was ranked in increasing order.

$$V = R - \frac{\left(P(P+1)\right)}{2} \quad \ldots \quad (3.5)$$

$$W = pq - V \quad \ldots \quad (3.6)$$

R is the sum of the ranks of the elements of the first sample (size p) in the combined series (size N), V and W are calculated from R, p, and q. V represents the number of times an item in sample 1 follows an item in sample 2 in the ranking. Similarly, W can be computed for sample 2 following sample 1. The M-W statistic U will be defined by the smaller of V and W. When N > 20 and p, q > 3, and under the null hypothesis that the two samples came from the same population, U is approximately normally distributed with mean and variance var (U),

$$\bar{U} = \frac{pq}{2} \quad (3.7)$$

$$Var(U) = \frac{pq}{N(N-1)}\left(\frac{N^3 - N}{12} - \sum T\right) \quad (3.8)$$

$$T = \frac{J^3 - J}{12} \quad (3.9)$$

Where T and J is the number of observations tied at a given rank. T is summed over all groups of tied observations in both samples of size p and q. Therefore, in this thesis the statistic u is used to test the hypothesis of homogeneity at 5 % significance level a by comparing it with the standard normal variate for that significance level.

$$u = \frac{U - \bar{U}}{\sqrt{Var(U)}} \quad (3.10)$$

3.3.1.3.Testing of outliers

Outliers are data points that depart significantly from the tread of the remaining data. The retention or deletion of this outlier can significantly affect the magnitude of statistical parameters computed from the data; especially for small samples procedures for trending outliers require judgment involving both mathematical and hydrological considerations. According to the (Jekel et al., 2014) if the station skew is bigger than +0.4 tests for high outliers are considered first; if station skew is less than -0.4, test for low outlier are considered first. Where the station skew is between -0.4 and +0.4, tests for both high and low outlier should be applied before eliminating any outliers from the data set. The following frequency equation can be used to detect high outliers.

$$Y_h = \bar{Y} + K_n S_y \quad (3.11)$$

Where: Y_h = High outlier threshold in log units,

K_n = Value read from table for sample size n

S_y = Standard deviation

$$S_y = \sqrt{\frac{\sum(Y_i - \bar{Y})^2}{n-1}} \quad , \quad Q_H = (10)^{Yh}$$

A similar equation can be used to detect low outliers

$$Y_L = \bar{Y} - K_n S_y \quad \ldots\ldots\ldots\ldots\ldots\ldots\ldots\ldots\ldots\ldots (3.12)$$

If the logarithms of the values in a sample are bigger than Yh in the above equation, then it is considered high outlier. Flood peaks considered high outliers should be compared with historic flood data and flood information at nearby sites. Historic flood data comprise information on unusually extreme events outside of the systematic record. According to the (Jekel et al., 2014) if information is available that indicates a high outlier is the maximum over an extended period of time, the outlier is treated as historic flood data and excluded from analysis. If useful historic information is not available to compare to high outliers, then the outliers should be retained as part of the systematic record.

3.3.2. Consistency checks and Adjustment of Rainfall Data

When dealing with inconsistent catchment rainfall data over time, it becomes necessary for hydrologists to correct or adjust the measured data to ensure a consistent record. Inconsistency in the data can arise from various factors such as changes in gauge location, exposure, instrumentation, or issues with the observational procedure. To address this problem, one widely applied technique is the Double-Mass Curve (DMC) analysis. The DMC analysis is a graphical method that compares the time trends of a particular station's record with those of nearby stations. It helps identify and adjust inconsistencies in the data. The DMC analysis involves plotting cumulative rainfall data for the station of interest against cumulative rainfall data from a reference station or a group of nearby stations. The cumulative rainfall is calculated by summing up the rainfall values over a specific period, such as yearly or monthly totals. By comparing the slopes and patterns of the two curves on the graph, inconsistencies or shifts in the time trends can be detected. If the curves of the station of interest and the reference station(s) exhibit similar patterns and slopes, it suggests a consistent record. However, if there are significant deviations or shifts between the curves, it indicates inconsistencies that need to be addressed.

The DMC analysis helps in identifying potential causes of inconsistency, such as changes in gauge location or exposure. Based on the analysis, adjustments can be made to the data by applying scaling factors or shifting the data to align the time trends with the reference station(s). This process helps create a more consistent record for further hydrological analysis and modeling. After the data of each station are arranged in descending order, the accumulative sums, station to be investigated and base station; are plotted against each other and line of best fit were sketched as shown on figure 3.4 below. The data series, which is inconsistent, adjusted to consistent values by proportionality.

$$P_{cx} = P_x * \frac{M_c}{M_a} \quad \text{.....(3.13)}$$

- Where Pcx is corrected precipitation at any time period and P_x is original recoded precipitation at time period
- M_c is corrected slope of double mass curve and M_a is original slope of the double mass curve

3.3.3. Goodness of fit test

This test helps to determine how well a specific distribution fits hydrological data and provide insights into the appropriateness of the chosen distribution. The D-index is a criterion used to select a suitable probability distribution for rainfall estimation.

It is calculated using Equation 3.14,

$$\text{D-index} = \left(\frac{1}{\bar{R}}\right) \sum_{i=1}^{6} [R_i - R_i{}^*] \quad \text{.....(3.14)}$$

Here, $\bar{R}$ is the average value of the series of the recorded rainfall, R_i (for i=1 to 6) are the six highest values in the series of recorded rainfall and $R_i{}^*$ is the estimated rainfall by probability distribution. The distribution having the least D-index is considered as the better suited distribution for rainfall estimation (USWRC 1981).

To determine the most suitable distribution, the D-index values are computed for different distributions, and the distribution with the lowest D-index is considered the best fit for rainfall estimation. In this case, the D-index values for various distributions were calculated and presented in Table 3.1. Upon analyzing the table, it can be observed that the D-index value obtained from the lognormal distribution is the lowest among the compared distributions, including normal, Log Pearson Type III, Gumbel EVI, Pearson

type III, and Gumbel distributions. This implies that the Gumbel EVI distribution is the best suited distribution for rainfall estimation based on the D-index criterion. The D-index provides a quantitative measure to assess the goodness-of-fit of different probability distributions for rainfall data. By comparing the D-index values, hydrologists can determine the distribution that closely matches the characteristics of the recorded rainfall data. In this case, the Gumbel EVI distribution exhibited the lowest D-index, indicating its superior fit for the rainfall data under consideration.

Table 3.1: D-index values of different distributions

Distributions	Normal	Log Pearson Type III	Log Normal	Pearson Type III	Gumbel EVI	Gumbel
D-index	0.84	1.02	0.99	0.83	1.02	2.82

3.4.Hydrological modeling using HEC-HMS model

HEC-HMS is a semi distributed model, in which data can be heterogeneous within basin but it is homogenous within sub-basins. The hydrological characteristics of the basin will be computed using the physical properties of all the sub basins for simulation. The Hydro-meteorological data and curve number for each sub basins will be required for simulation of the model. To perform rainfall-runoff modeling with HEC-HMS, several input files are required:

- Background Map File: This file provides the spatial information and characteristics of the study area. It includes data such as the boundaries of the catchment, topography, land use, and other relevant features.
- Basin Model File: The basin model file contains the hydrological characteristics and parameters of the catchment being modeled. It includes information on soil types, land use categories, vegetation, and flow routing methods.
- Gage File: The gage file includes observed precipitation and/or stream flow data, which are used for calibration and validation of the model. This data is typically obtained from rain gauges or stream gauges located within the study area.
- Met File: The met file contains meteorological data required for the rainfall-runoff simulation. It includes information such as precipitation, temperature, humidity, wind speed, and solar radiation. These data are used to estimate actual

evapotranspiration and calculate potential evapotranspiration using different methods.

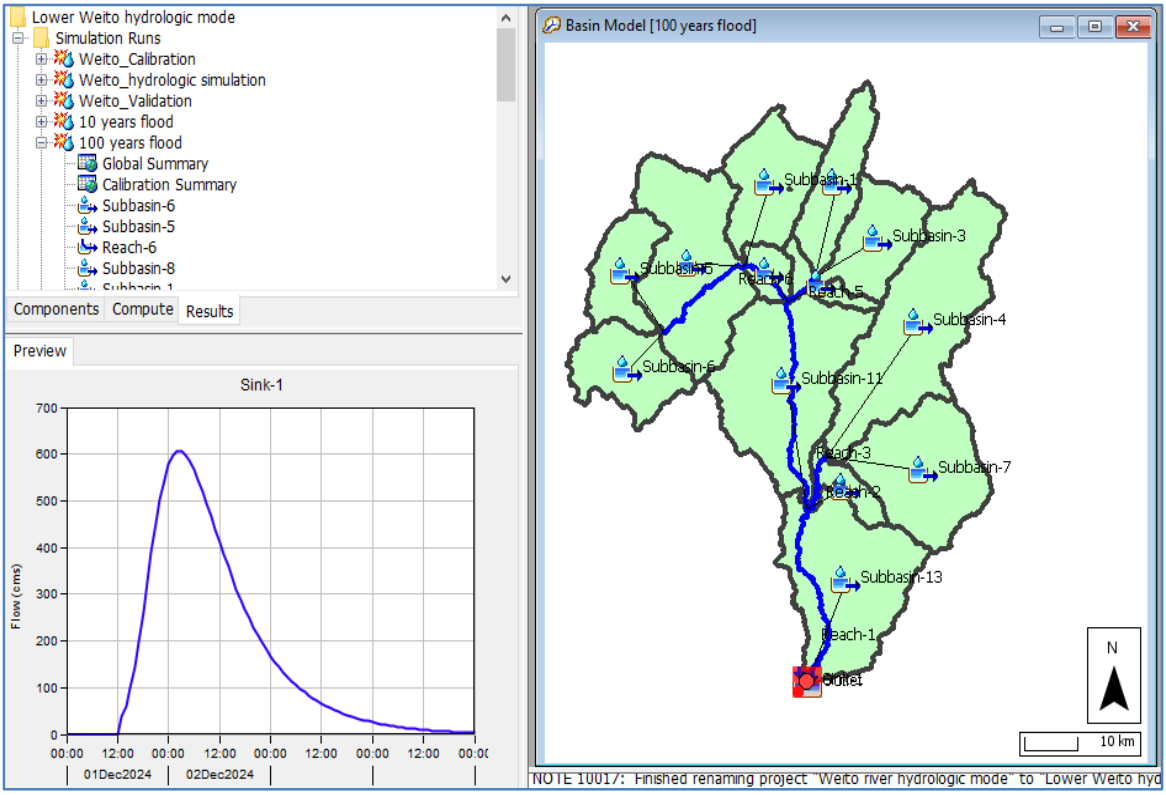

Figure 3.5: Weito river watershed in HEC HMS model.

HEC–HMS consists of different methods for precipitation loss modeling; The SCS Curve Number (SCS-CN) model is a commonly used method within the HEC-HMS software for estimating excess precipitation or direct runoff from a storm event. It was developed by the Soil Conservation Service (SCS), now known as the Natural Resources Conservation Service (NRCS), in 1972. The SCS-CN model takes into account various factors such as cumulative precipitation, soil type, vegetation, and antecedent moisture condition of the watershed to estimate the depth of excess rainfall or direct runoff.

The computation of excess precipitation or direct runoff using the SCS-CN model is based on the following equation:

$$Q = \frac{(P-0.2S)^2}{P+0.8S} \quad \text{(3.16)}$$

Where:

Q = Depth of excess precipitation or direct runoff (in inches)

P = Cumulative precipitation (in inches)

S = Potential maximum retention after runoff begins (in inches)

In the SCS Curve Number (SCS-CN) model, the potential maximum retention (S) is related to the Curve Number (CN) and can be calculated using the following equation:

$$S = \frac{25400 - 254\,CN}{CN} \quad \text{(3.17)}$$

Where:

S = Potential maximum retention after runoff begins (in inches)

CN = Curve Number

In a watershed with different land uses and soil types, a composite Curve Number (CN) can be calculated to estimate the runoff volume. The composite CN represents an average value that considers the contributions of individual watershed subdivisions with homogeneous land use and soil type. The equation to calculate the composite CN is as follows:

$$CN_{composite} = \frac{\sum A_i\, CN_i}{\sum A_i} \quad \text{(3.18)}$$

Where:

CN_composite = Composite Curve Number used for runoff volume estimation

i = Index of each watershed subdivision with homogeneous land use and soil type

CNi = Curve Number of the watershed subdivision i

Ai = Drainage area of the subdivision i

The resulting value, CN_composite, represents the average Curve Number for the entire watershed, taking into account the variations in land use and soil type. This composite CN can be used in the SCS-CN model or other runoff volume estimation methods to simulate the runoff process and estimate the total runoff volume more accurately. The model allows the transformation of excess precipitation into direct runoff. The SCS (Soil Conservation Service) unit hydrograph model is commonly used as a transform model in

the Hydrologic Engineering Center's Hydrologic Modeling System (HEC-HMS) for certain watersheds due to its simplicity, wide applicability, and historical significance.

In SCS unit hydrograph model, which is used as a transform model to convert excess precipitation into point runoff, the following relationships and equations are used:

Relationship between UH peak (Up) and time to UH peak (Tp):

$$U_p = C\frac{A}{T_p} \quad \text{(3.19)}$$

Where:

Up = Peak discharge of the unit hydrograph (in cubic feet per second)

A = Watershed area (in acres)

C = Conversion constant (2.08) - This constant is used to convert the Up to the desired units based on the unit of A (acres) and Tp (hours)

Tp = Time to the UH peak (in hours)

This relationship allows for the estimation of the peak discharge of the unit hydrograph based on the watershed area and the time to the peak. Relationship between the time to UH peak (Tp) and the duration of the unit of excess precipitation (Δt) and basin lag (tlag):

$$T_p = \frac{\Delta t}{2} + t_{lag} \quad \text{(3.20)}$$

Where:

Δt = Duration of the unit of excess precipitation (in hours)

Tlag = Basin lag (in hours)

Basin Lag time in hours for each sub-basin was computed using equation (3.11) (Arlen, 2000) and then converted to minutes.

$$Lag = \frac{L^{0.8}\,(S+1)^{0.7}}{1900 * Y^{0.5}} \quad \text{(3.21)}$$

Where S = Maximum retention

Lag = basin lag time (hours)

L= hydraulic length of the watershed (longest flow path)

Y = Basin slope (%).

The model includes several methods for channel flow routing. Among those models, the Muskingum model for flood routing was selected for this study due to the availability of required data. The Muskingum method uses a simple finite difference approximation of the continuity equation:

$$\left(\frac{I_{t-1}+I_t}{2}\right)-\left(\frac{O_{t-1}+O_t}{2}\right)=\left(\frac{S_t+S_{t-1}}{\Delta t}\right) \qquad (3.22)$$

Storage in the reach is modeled as the sum of prism storage and wedge storage. The storage is defined by the model as:

$$S_t = KO_t + KX(I_t - O_t) = K[XI_t + (1-X)O_t] \qquad (3.23)$$

Where K = travel time of the flood wave through routing reach, and X = dimensionless weight ranging from 0 to 0.5. The quantity $XIt + (1 - X)\ Ot$ is a weighted discharge. When the storage in the channel is controlled by downstream conditions, such that storage and outflow are highly correlated, X=0.0. Thus, $S = KO$ and it is the linear reservoir model. If X=0.5, the inflow, and outflow have the same weight which means that the wave does not attenuate when moving through the reach. By substituting equation (2.9) in (2.8) and rearranging to isolate the unknown values at time t, we have:

$$O_t = \left(\frac{\Delta t-2KX}{2K(1-X)+\Delta t}\right)I_t + \left(\frac{\Delta t+2KX}{2K(1-X)+\Delta t}\right)I_{t-1} + \left(\frac{2K(1-X)-\Delta t}{2K(1-X)+\Delta t}\right) \qquad (3.24)$$

3.4.1. Basin characteristics

Basin characteristics refer to the physical and hydrological properties of a watershed or catchment area. These characteristics play a crucial role in understanding and modeling the behavior of the basin's hydrological processes. Some important basin characteristics include Curve Number (CN), Basin Lag Time, basin area, Basin Slope, Potential Maximum Retention (S).

Table 3.2: Basin parameters of Weito watershed

Sub basins	L(Km)	Basin slope	Basin Area(Km2)	CCN	Tlag(Min)	Ia(mm)
Subbasin-1	40.69154	0.20635	307.19	74.1	251.06	17.783
Subbasin-2	45.75015	0.17545	238.15	69.9	335.87	21.91157
Subbasin-3	33.9336	0.27157	265.38	73.6	191.6	18.19796
Subbasin-4	79.51987	0.33501	710.9	71.3	363.75	20.445
Subbasin-5	36.23046	0.37356	200.09	67	206.14	25.021
Subbasin-6	37.98082	0.32653	261.25	67.2	227.91	24.823
Subbasin-7	45.77885	0.21271	462.18	75.8	258.91	16.26
Subbasin-8	39.62226	0.33659	579.36	69.7	216.97	22.059
Subbasin-9	25.5034	0.16774	71.881	74.7	188.17	17.198
Subbasin-10	20.86189	0.30198	74.661	75	118.43	16.933
Subbasin-11	65.12155	0.20337	660.29	73.4	375.62	18.427
Subbasin-12	31.84098	0.09762	84.732	79.8	253.06	12.8508
Subbasin-13	66.95853	0.21797	598.63	70.2	405.08	21.572

3.4.2. Calibration and Validation of the Model Parameters

After the model setup is completed for HEC-HMS model, the next step is to run the model and analysis the simulated result. The applicability of the model for intended purpose should be evaluated through the process of sensitivity analysis, calibration and validation (White and Choubey, 2005). For further analysis of the result, model calibration involves modification of input parameters and comparison of predicted output with observed values until the defined objective function is achieved (James and Burges, 1982). And the calibration was carried out by trial and error where model parameters are manually or automatic calibration. In order to utilize the calibrated model for estimating the effectiveness of future potential management practices, the model tested against an independent set of measured data. This testing of a model on an independent set of data set is commonly referred to as model validation. As the model predictive capability was demonstrated as being reasonable in both the calibration and validation phases, the model is used for future predictions under different management scenarios (Ashenafi, 2013). Daily rainfall and stream flow data from 1990 to 2015 were used for calibration and validation of the model. The data from 1990 to 2006 were used during calibration and from 2007 to 2015 was used during validation.

3.4.3. Model Performance Evaluation Criteria

Performance measurement allows for visual comparison of data from simulated and measured output responses, helps to identify model bias, identify variations in peak timing and magnitude (e.g. peak flows) and recession curve shape, etc. (Moriasi, 2015). The performance of the HEC–HMS model was evaluated on four performance assessment parameters. These are Nash Sutcliff Efficiency (NSE), determination coefficient (R^2), root mean square error (RMSE) and percent biass (PBIAS).

Nash–Sutcliffe model efficiency coefficient (NSE): used to analyze the correlation between simulated and observed hydrological data. It can range from -∞ to 1. An efficiency of 1 indicates a correct match of simulated (modeled) discharge to the measured (observed) data. The efficiency of 0 shows the model prediction is as perfect as of the average of the observed data, whereas the efficiency less than zero occur when the observed average is a better predictor than the modeled or, in another word, when the residual variances (expressed by a nominator) is greater than the data variances (expressed by a denominator). Essentially, the closer the model efficiency is to 1, the more accurate it is. The disadvantage of this efficiency criterion is an overestimation of the model performance during peak-flows and an underestimation during the low-flow condition. It can be expressed as follow:

$$\mathrm{NSE} = 1 - \frac{\sum_{i=1}^{n} (Q_{si} - Q_{oi})^2}{\sum_{i=1}^{n} (Q_{oi} - \bar{Q}_o)^2} \quad \text{.....(3.25)}$$

Where, Q_{si} - Simulated flow value at the i^{th} time interval, Q_{oi} - Observed flow value at the i^{th} time interval, $\bar{Q}_o$ - Mean observed flow value

Coefficient of Determination (R^2): The coefficient of determination is a measure of the proportion of variances of the forecasted outcomes. It estimates how well the dispersion of the measured data is predicted by the model. With a value of 0-1, the coefficient of determination is computed as the square of the correlation coefficients (R) between the sample and forecasted (predicted) data. The coefficient of determination indicates how well a regression model fits the data. A value of 1 shows every point on the regression lines fit the data; a value of 0.5 shows only half of the variations are discussed by the regression. A zero coefficient of determination (R^2) indicates that the dependent variable

cannot be forecasted from the independent variable. The equation of coefficient of determination can be expressed as follow:

$$R^2 = \frac{\sum_{i=1}^{n}(Q_{si}-\overline{Q}_s)(Q_{oi}-\overline{Q}_o)^2}{\sum_{i=1}^{n}(Q_{si}-\overline{Q}_s)^2 \sum_{i=1}^{n}(Q_{oi}-\overline{Q}_o)^2} \quad \text{(3.26)}$$

Where Qsi - Simulated flow value at the ith time interval, Q_{oi} - Observed flow value at the ith time interval, $\overline{Q}_o$ - Mean observed flow value, $\overline{Q}_s$ - Mean Simulated flow value.

3.4.4. Flood Frequency Analysis

Flood Frequency Analysis (FFA) is a critical statistical method used to understand the characteristics and magnitude of peak flows in rivers or floodplains. It provides a probability model curve that relates the frequency of occurrence of a flood peak to its magnitude. This analysis is based on historical flood data and observations collected over a specific period. After calibrating and validating the hydrological model using observed flow data, the next step was to estimate the maximum annual rainfall for durations other than the available 24-hour data. Thus, by analyzing the peak annual rainfall data recorded over a period of 31 years (1990-2021), FFA allows for the estimation of return periods. The ERA Drainage Manual 2013 introduced an equation that was utilized to estimate the maximum annual rainfall for various durations based on the available 24-hour maximum rainfall data. This equation assumes a relationship between the 24-hour maximum rainfall and the maximum rainfall for different durations. By applying this equation, the maximum annual rainfall values for selected durations, such as 1-hour, 2-hour, 6-hour, or any other desired duration, were calculated. These estimates were derived from the observed 24-hour maximum rainfall data. Using the provided equation from the ERA Drainage Manual 2013, the annual maximum rainfall depths were computed for each selected duration. This allowed for the estimation of rainfall intensities for different durations, which is crucial for understanding the potential for intense rainfall events and their impact on hydrological processes. It is important to note that the specific equation from the ERA Drainage Manual 2013 is likely based on extensive analysis of rainfall data and regional characteristics. The coefficients or formulas within the equation take into account factors such as climate patterns, geographical location, and statistical analysis of rainfall data. By utilizing this equation, it becomes possible to estimate the maximum annual rainfall depths for various durations,

$$R_{Rt} = \frac{t}{24}\,\frac{(b+24)^n}{(b+t)^n} \quad \text{..... (3.27)}$$

Where:

R_{Rt} = Rainfall depth Ratio R_t: R_{24}

R_t = Rainfall depth in a given duration's t.

R_{24}= 24 hr. rainfall depth b and n = coefficients b=0.3 and n= (0.78-1.09).

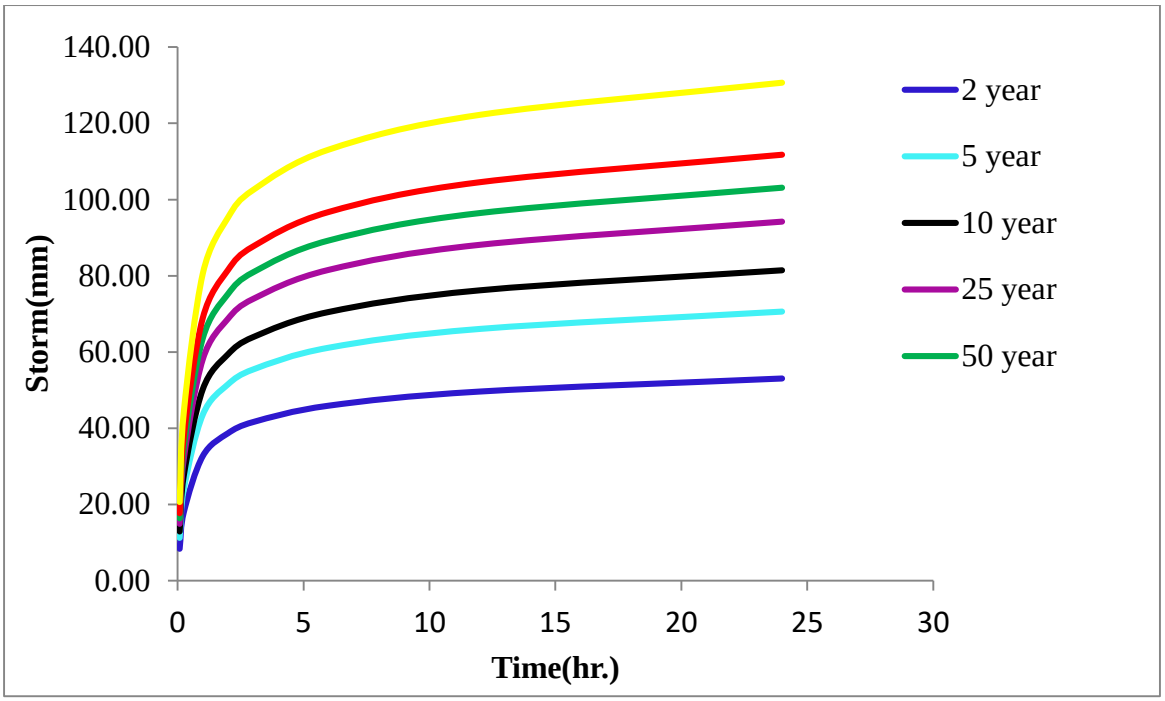

Figure 3.6: Frequency storm depth

3.5. Hydraulic Modeling Using HEC RAS model

The full unsteady flow equations have the capability to simulate the widest range of flow situations and channel characteristics. The basic data requirements for hydraulic routing techniques include: flow data, channel geometry, roughness coefficients, and the boundary conditions.

Unsteady flow analysis was used to evaluate the downstream attenuation of the flood wave, providing a more accurate estimate of flood magnitude and velocity at critical locations.

3.5.1. Mesh Generation

The accuracy of the HEC RAS result is dependent on the terrain of the study area. Mesh of narrow size for good accuracy was developed for simulation used in geometric data editor. In the current study area, mesh size of 20m * 20 m was used for simulation. Figure below shows the mesh generated in geometric data window of HEC-RAS model.

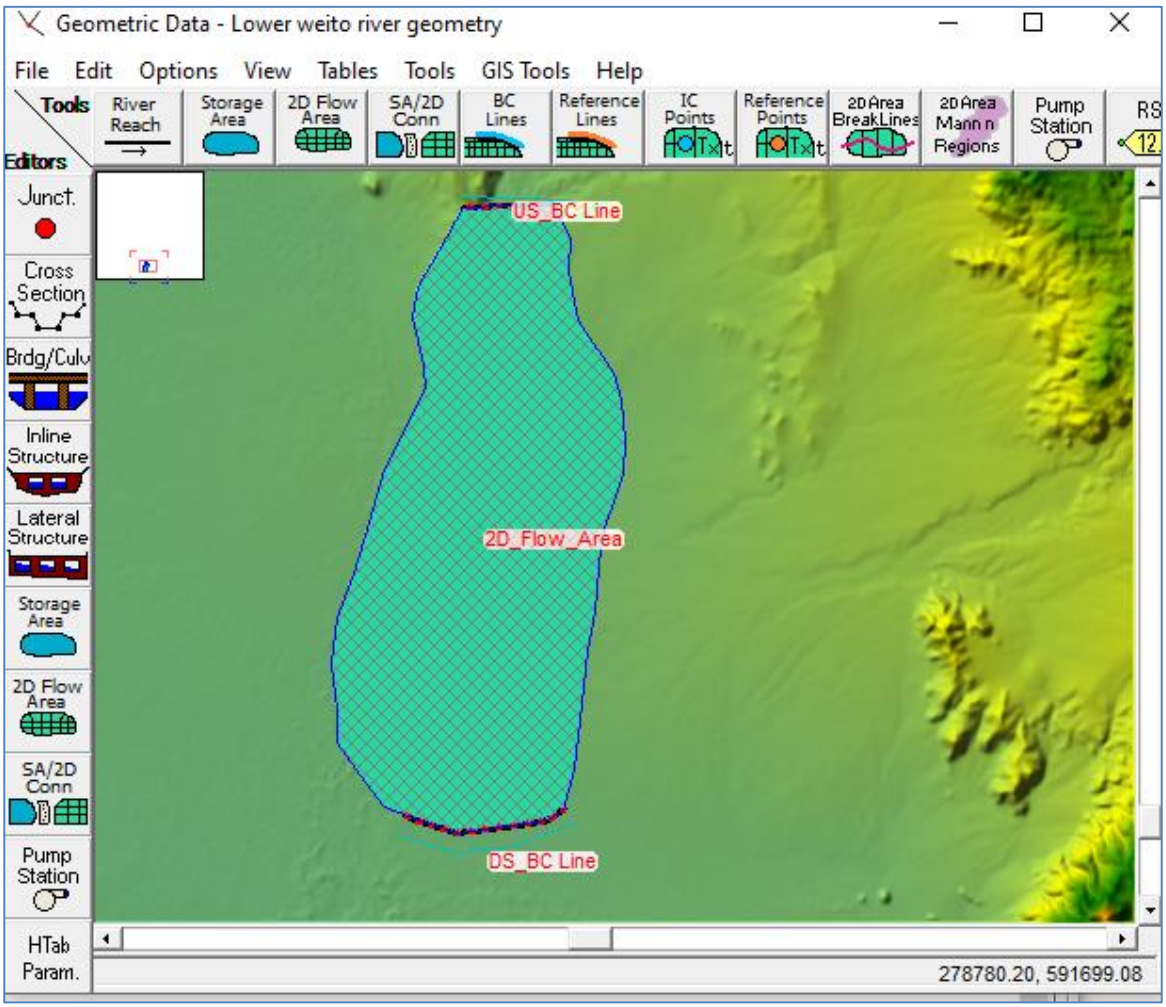

Figure 3.7: Mesh generation within 2D Area

3.5.2. Manning's roughness coefficient

The manning's roughness coefficient is used to reflect the resistance to flow from bed material. The roughness of a surface affects the characteristics of runoff, whether the water is on the surface of the watershed or in the channel. With respect to the hydrologic cycle, the roughness of the surface retards the flow. For overland flow, increased roughness delays the runoff and increase the potential for infiltration. Reduced velocities associated with increased roughness should also decrease the amount of erosion (Gilley et al., 1991). All hydraulic computations involving flow in open channels require an

evaluation of the roughness characteristics of the channel. The ability to evaluate roughness coefficients must be developed through experience. One means of gaining this experience is by examining and becoming familiar with the appearance of some typical channels whose roughness coefficients are known (Bahramifar et al., 2013). Common methods of estimating Manning's roughness coefficients for stream channels, includes use of published *n*- value data, comparison with photographs of channels for which *n* values have been computed, and *n* - value equations (Coon, 1997). A Manning *n* will be assigned in accordance with a simple land cover classification that will be manually created from parcel outlines and digital orthophotos, using Chow's (1959) tabular *n* values for similar land characteristics (Gallegos et al., 2009). The roughness Manning *n* values for different land uses are provided on Chow's (1959). It could also be selected based on reviewing the site visit, photographs and aerial imagery of channel and flood plain areas (Asnaashari et al., 2014). The Manning's coefficients for the channel and overbank areas have been estimated based on the field investigation (Changzhi et al., 2014).

3.5.3. External 2D Flow Area Boundary conditions unsteady simulation

Boundary conditions both at the upstream and downstream ends of study area are needed for the model in flood routing. There are five types of external boundary conditions that can be linked directly to the 2D flow areas. These are Flow Hydrograph, Stage hydrograph, Normal depth, Rating curve and Precipitation boundary condition. The Normal depth and rating curve boundary condition can only be used at locations where flow will leave a 2D flow area. The flow and stage Hydrograph boundary condition can be used for putting flow into or taking flow out of a 2D flow area.

Unsteady flow data used as a boundary condition in this study are: 10years inflow hydrograph, 25 years inflow hydrograph, 50 years inflow hydrograph, 100 years inflow hydrograph and Normal depth. Normal depth is used as a downstream boundary condition. Normal depth can only be used as a downstream boundary condition for an open-ended. To use normal depth, it is required to enter a friction slope for the reach in the vicinity of the boundary condition. The slope of the water surface is often a good estimate of the friction slope. In addition to the boundary condition, initial condition should be established at the beginning of the unsteady flow simulation. Initial condition consists of flow and stage information at each of the cross sections, as well as elevations for any storage areas defined in the system. Once the terrain development steps are

complete, the 2D simulation is executed in HEC-RAS. The software solves the 2D Saint-Venant equations using the selected computational method (e.g., Full Momentum or Diffusion Wave) to simulate the flow behavior and water surface elevations within the defined area.

3.5.4. Post Processor

The post processor is used to compute detailed hydraulic information for a set of user specified time lines during the unsteady flow simulation period. The Post processor compute detail output for a maximum stage water surface profile. The computation setting area of the unsteady flow analysis window contain the computation interval, hydrograph output interval, mapping output interval and detailed output interval (Eichert, 1964). The computation interval is used in the unsteady flow calculation. This is one of the most important parameters entered into the model and selected with care due to it affects the simulation. Firstly, the interval should be small enough too accurately to describe the rise and fall of the hydrograph being routed. In this study it is taken with 20 seconds. In my study 30 minutes is used as hydrograph output interval. The detailed output interval field allows the user to write out profiles of water surface elevation and flow at a user specified interval during the simulation. One hour is used for detailed output interval. For medium to large rivers, the courant condition may yield time steps that are too restrictive (a larger time step could be used and still maintain accuracy and stability). The smaller time step is needed when there is lateral weirs/spillways and hydraulic connections between storage areas and the river system. Computational time step stability and accuracy can be achieved by selecting a time step that satisfies the courant condition. Remember that for Hydraulic models, typical time steps are in the range of 1- 60 seconds due to the very fast flood wave velocities (Eichert, 1964).

$$C = \frac{V\Delta T}{\Delta X} \leq 2\ (with\ \alpha \max C = 5) Or\ \Delta T \leq \frac{2\Delta X}{V}\ (with\ C = 2) \ldots\ldots\ldots\ldots (3.28)$$

Where: C=Courant Number; ΔT =Computation time step(s);

V= Flood wave velocity (wave celerity) (m/s); ΔX=Average cell size (ft)

3.5.5. 2D energy equation (Mass Conservation)

The continuity equation and momentum equation are the main scientific basis for unsteady flow analysis. The continuity equation is as follow: (Eichert, 1964)

$$\frac{\partial \mathrm{A}}{\partial \mathrm{t}} + \frac{\partial \mathrm{Q}}{\partial \mathrm{s}} - \mathrm{q} = 0 \quad \ldots\ldots\ldots\ldots\ldots\ldots\ldots\ldots\ldots\ldots\ldots\ldots\ldots\ldots\ldots\ldots\ldots\ldots\ldots\ldots\ldots\ldots\ldots\ldots \quad (3.29)$$

Where, A = flow area, m2;

Q = volume of flow, m3/s;

q = the lateral inflow per unit length,

m2/s;

t = time variable, s;

s = spatial distance along the direction of

flow, m.

3.5.5.1.Diffusion-Wave equation

And one form of the Diffusion-Wave momentum equation is as follow (Eichert, 1964). $\frac{\partial A}{\partial t} + \frac{\partial QV}{\partial s} + gA\left(\frac{\partial z}{\partial s} + sf\right) = 0$ ……………………………………………………….…….…..(3.30)

Where, V = flow velocity, m/s;

z = elevation of water surface, m;

g = gravitational acceleration, m/s2;

Sf = friction slope.

$$sf = \frac{Q^2 n^2}{R^{\frac{4}{3}} * A^2} \quad \ldots\ldots\ldots\ldots\ldots\ldots\ldots\ldots\ldots\ldots\ldots\ldots (3.31)$$

Where, n = manning's roughness coefficient; R = hydraulic radius, m

3.6. Flood Hazard map

Flood hazards are multifaceted and encompass various dimensions that need to be considered by flood managers. These dimensions include the where, when, how long-lived, and how much adjustment occurs in relation to flood events. To identify and communicate the potential dangers associated with floods, flood hazard maps are created. These maps take into account the depth and velocity of floodwaters, as the combined effect of these factors determines the severity of the hazard. Geographic Information System (GIS) software is commonly used to map flood hazards and provide visual representations of the areas at risk. These maps assist in decision-making processes regarding land use, emergency planning, and the allocation of resources for flood management and mitigation efforts.

3.7. Flood vulnerability map

A flood vulnerability map is a spatial representation that depicts the areas at risk of flooding and their corresponding levels of vulnerability. It combines various geographic and socio-economic factors to assess the potential impacts of floods on different areas. In flood vulnerability analysis, it is essential to consider different indicators that provide information about exposure, susceptibility, and resilience. These indicators help assess the potential impact

and vulnerability of an area to flood events. The collected data for these indicators are then arranged in increasing order to determine the values for the Vulnerability Index.

- Exposure indicators (Xi) represent the elements or factors present in an area that are at risk of being affected by floods. These can include human settlements, infrastructure, cultural heritage sites, agricultural fields, and other relevant components. The exposure index (I) is obtained based on the functional relationship of these indicators, which can be determined using a specific formula.
- Susceptibility indicators (Xi) reflect the potential of a system or its components to be harmed or negatively impacted by flood events. These indicators consider factors such as fragility, social and economic weaknesses, and unfavorable conditions. The susceptibility index (I) is calculated based on the functional relationship of these indicators, which may involve using a formula specific to the study. Resilience represents the ability of a system or community to adapt, cope with, and recover from flood events. It is a measure of the capacity to absorb and mitigate potential damages caused by floods.
- Resilience indicators are important in understanding the system's ability to withstand and recover from flood impacts.

The vulnerability of a system to flood events can be expressed with the following general equation (Balica, 2007, p 37). This equation is used in the present study to compute Flood Vulnerability Index (FVI).

FVI = Exposure Index* Susceptibility Index- Resilience Index……(3.32)

. Based on the literatures reviewed, field visit and focused group discussion (FGD) with key informants in the study area, the socio-economic indicators such as, Flood depth, Flood velocity, flood duration, slope, DEM and land-use, are selected in this study as they so much influence the vulnerable nature of the study area.

3.8. Flood Risk Analysis

Flood risk analysis is a process of assessing and evaluating the potential risks associated with flooding in a particular area. For this study, flood hazard and flood vulnerability will be developed, flood risk then developed by overlaying flood hazard map and food vulnerability map. According to Zimmermann, 2005) the conventional expression of risk is,

Risk=Hazard * Vulnerability ……..……...……(3.33)

4. RESULT AND DISCUSSION

4.1. Rainfall-runoff simulation using HEC-HMS Model

The hydrologic simulation of the lower Weito watershed involved the calibration and validation of the model using stream flow and precipitation data. The calibration period spanned from 1990 to 2001, while the validation period covered the years 2002 to 2007. Figure 4.1 below shows a visual representation of the simulated and observed flows during the calibration and validation periods. This figure displays the modeled stream flow values alongside the observed flow values for comparison and evaluation. By examining the plot, one can assess the accuracy and performance of the model during both the calibration and validation periods.

4.1.1. Model Calibration

In the current study, the model calibration was done by using the sensitive parameters to achieve a goodness of fit between simulated and observed data. The auto-calibration (through optimization trials) available in the HEC-HMS model was used for optimizing the model parameters. Observed daily rainfall and stream flow data from 01 January, 1990 to 31 December, 2002 were used in the calibration process. The data set chosen to carry out the calibration and validation process depends on the availability of the data. The accuracy of the model can be measured by considering the R^2 values as well as the NSE values. R^2 and NSE values approaching 1 indicate a better model and values closer to 0 consider a worse model.

According to Moriasi et al. (2007), the performance of the model during calibration periods can be classified as "very good." Moriasi et al. (2007), suggest that for a model to be considered very well, the values of Nash-Sutcliffe Efficiency (NSE) and Coefficient of determination (R^2) should fall between 0.75 and 1.0. In this study, the values of both NSE and R^2 were 0.77 and 0.782 respectively which was greater than 0.75 for the calibration period, and this indicates a high level of agreement between the simulated and observed data. Table 4.1 below shows model performance evaluation for calibration periods. The Root Mean Squared Error (RMSE) was 1.33. Moriasi et al. (2007) suggested the RMSE value of less than 5 indicates a very good model performance. In this case, the calibration RMSE values fall within this range. Similarly, the percent bias (PBIAS) was 0.67 and the PBIAS value less than +10 suggests a very good model performance (Moriasi et al. (2007).

Table 4.1: model performance measures during the calibration

Measure	Value	Performance rating
Coefficients of determination (R2)	0.82	Very good
Nash Sutcliffe coefficients (NSE)	0.77	Very good
Root Mean Square Error (RMSE)	1.33	Very good
Percent Biass	0.67	Very good

The runoff and observed hydrograph results from the calibration process was shown in Figure 4.1 below. The final results of hydrological modeling displayed a very good fit between the simulated and observed hydrographs as shown in Fig. 4.1. The correlation between simulation and observed flow as scatter plot during the calibration at Weito bridge station was shown in Figure 4.2 below.

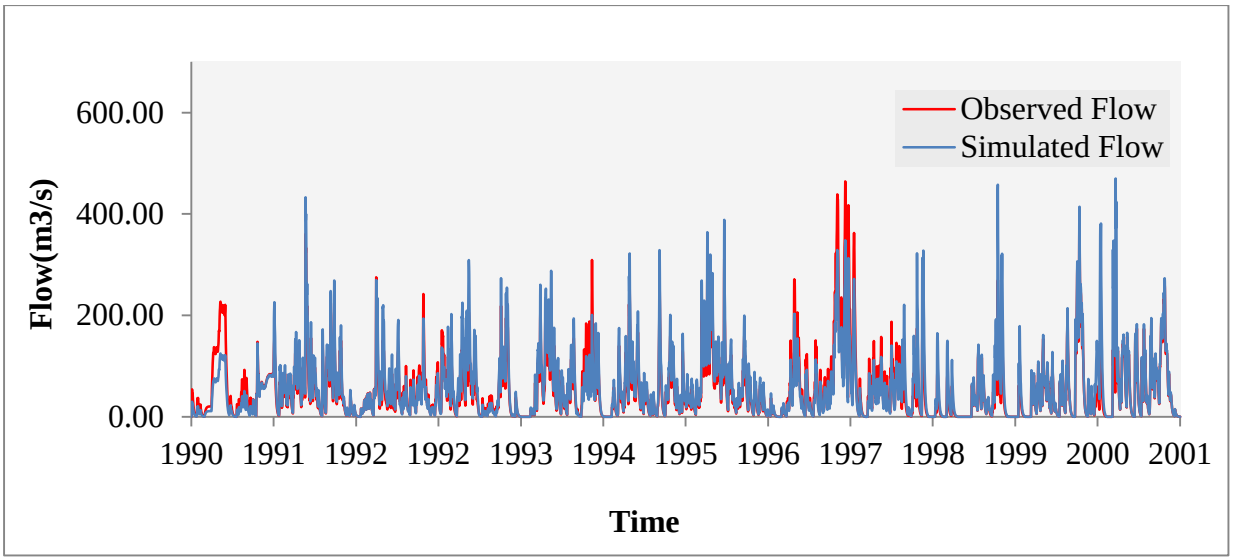

Figure 4.1: Comparison of the simulated and observed hydrograph after calibration

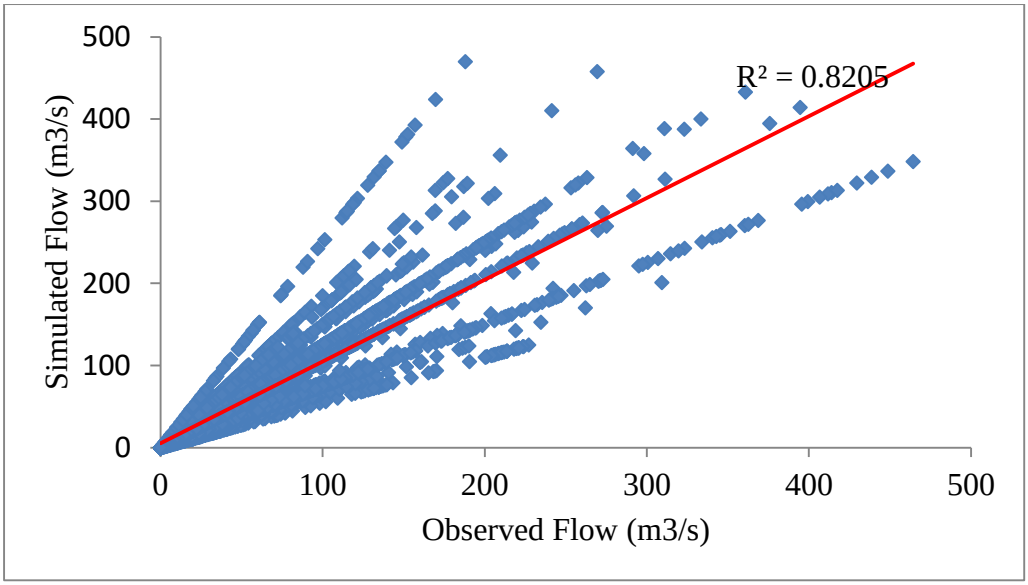

Figure 4.2: Correlation between simulated and observed flow during calibration

4.1.2. Model Validation

For validating the model, data from 2002 to 2007 were used in which the parameters obtained during the calibration was used for validation. Validation results obtained were better than the calibration results. The study conducted by Tassew et al. (2019) also gives similar results, which was the result from validation was better than the calibration, when using HEC-HMS model in simulating rainfall-runoff model in the Lake Thana basin. The results obtained during the validation process at the Weito bridge station shows that R^2 values of 0.78 and NSE of 0.75. These results can be judged as very good performance (NSE >0.75) (Moriasi et al. 2015). The performance of the model and comparison between peak flow and predicted peak flow during the validation process showed in table 4.2 below. The correlation between simulation and observed flow during the validation was shown in Figure 4.3 below. Generally, during validation, a good simulation was made between the estimated and observed values.

Table 4.2: Model performance values during validation

Measure	Value	Performance rating
Coefficients of determination(R2)	0.78	Very good
Nash Sutcliffe coefficients(NSE)	0.75	Very good
Root Mean Square Error(RMSE)	1.8	Very good
Percent Biass	1.2	Very good

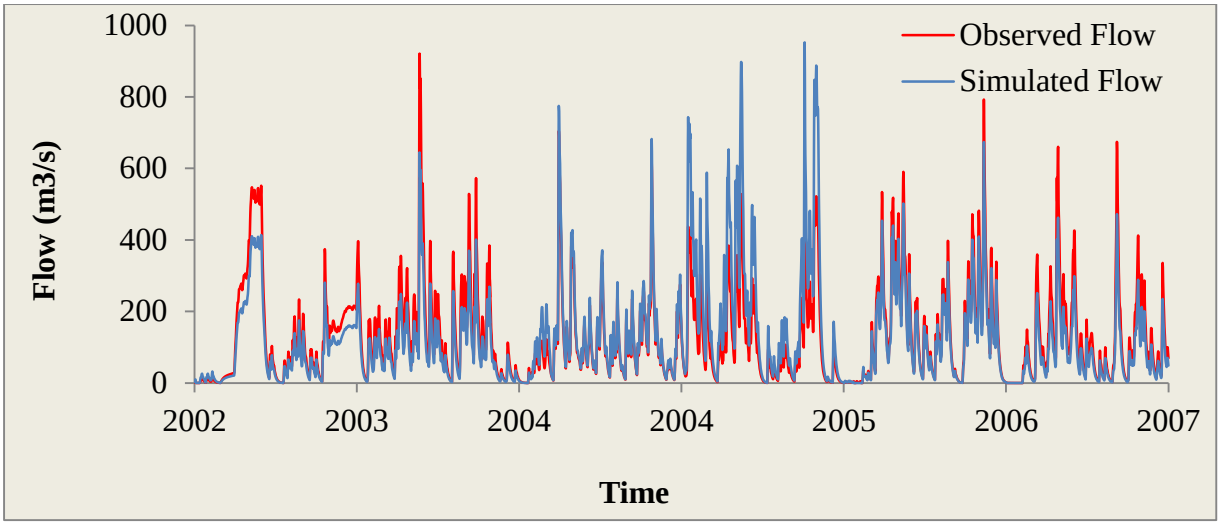

Figure 4.3: Comparison of the simulated and observed hydrograph after validation

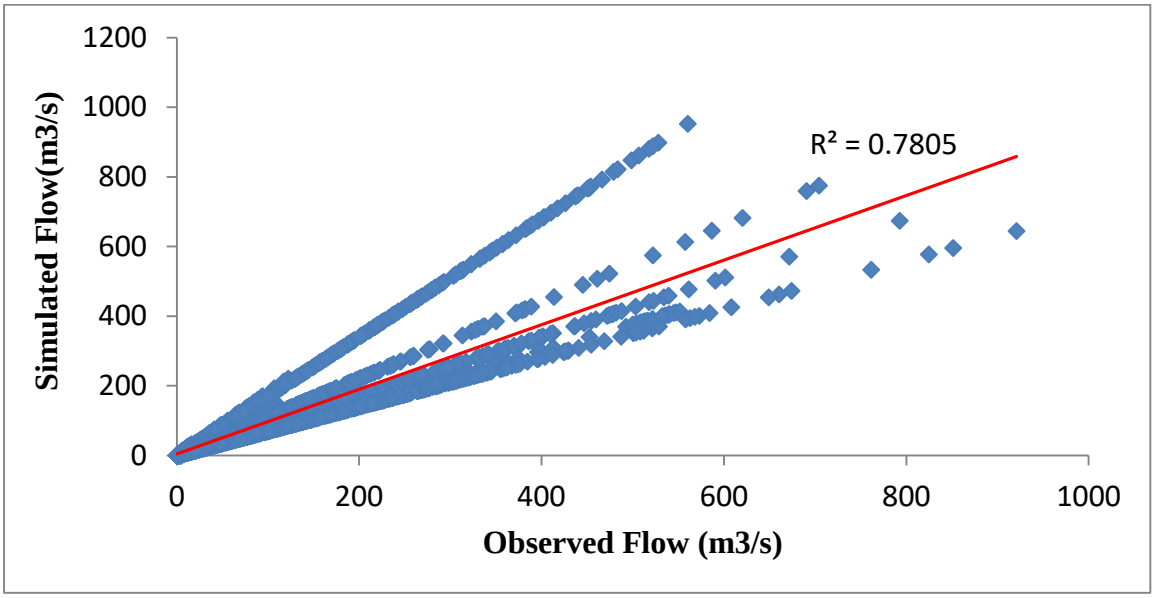

Figure 4.4: Correlation between observed and simulated flow during validation

4.1.3. Estimation of Maximum Flood hydrographs for different frequency

The flood frequency curve and the corresponding storm depths were used to estimate flood hydrographs for different return periods in the Lower Weito River. The flood hydrographs represent the variation in flow over time during different storm events of varying frequencies. The minimum peak flow for a 2-year return period with 24-hour storm duration was estimated to be 77.9m^3/s. This indicates that, on average, the Lower Weito River experiences a relatively low flow during such events. Conversely, the maximum peak flow occurs with a 100-year frequency storm, also lasting for 24 hours, with a flow value of 606.2m^3/s. This suggests that

the Lower Weito River experiences significantly higher flow during extreme flood events. Figure 4.6 illustrates the flood hydrographs estimated using the HEC HMS model for various return periods. These hydrographs provide a visual representation of how the flow in the Lower Weito River varies over time during different storm events of different frequencies. They demonstrate the rising and falling of water levels and the corresponding flow rates during these flood events. To further analyze the flood behavior, the flood hydrographs obtained from the HEC HMS model were utilized as upstream boundary conditions in the HECRAS model for unsteady flood simulation. This allows for a more detailed examination of the flood behavior, including the spatial distribution of floodwaters, flood depths, and velocities throughout the Lower Weito River system.

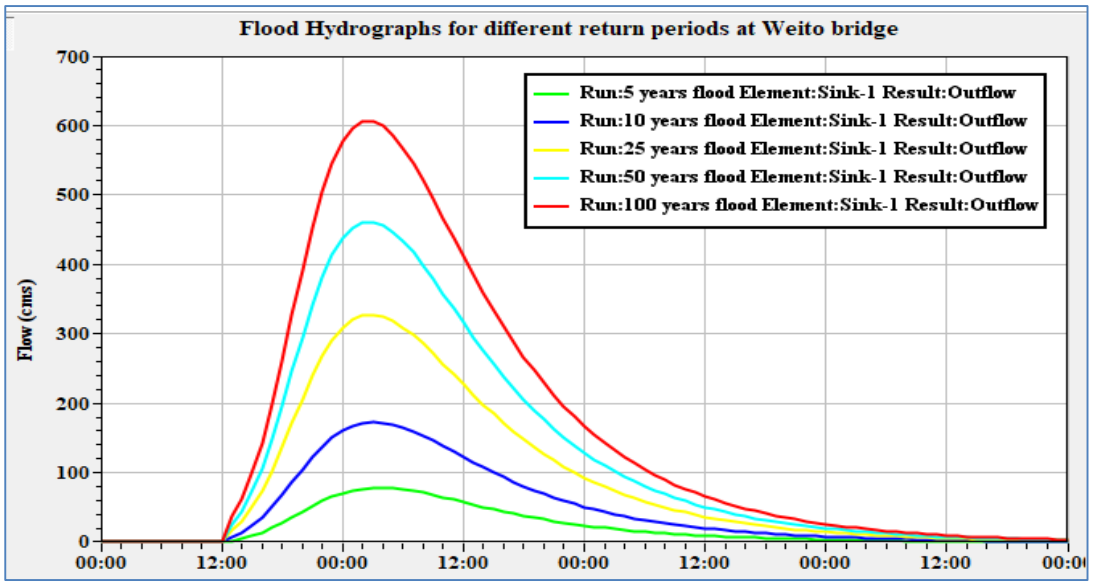

Figure 4.5: Maximum flood hydrographs for different return period at Weito bridge station

4.2.Sensitivity analysis in HEC-RAS model

4.2.1. Sensitivity of WSE to change of manning's roughness at critical location

The result of sensitivity analysis for manning's roughness shows the variation of WSE values along the selected flood plain for different roughness coefficients. The figure likely demonstrates that as the roughness coefficient increases, the WSE profile becomes increasingly non-uniform, indicating a gradual variation in flow conditions. This suggests that the WSE profile is sensitive to changes in the Manning's roughness coefficient. By conducting this sensitivity analysis, the researcher aimed to understand how changes in Manning's roughness coefficient affect the accuracy and reliability of the simulated water surface profiles. This

information is valuable for improving the modeling accuracy and understanding the hydraulic behavior of the river system under different flow conditions. Similar works have indicated the importance of sensitivity analyses with Manning's roughness in flood modeling. For instance, a study on the sensitivity of roughness coefficients in flood modeling emphasized that variations in roughness significantly affect flow velocity and water surface elevation, thereby impacting flood extent and propagation characteristics Additionally, research utilizing advanced hydrodynamic models like HEC-RAS and MIKE 21 has demonstrated that roughness variations are crucial for accurately simulating flood behavior and assessing floodplain risks [2]. These studies collectively underscore the necessity of robust sensitivity analyses to quantify the uncertainty introduced by roughness assumptions, ultimately leading to improved flood risk assessments and infrastructure planning.

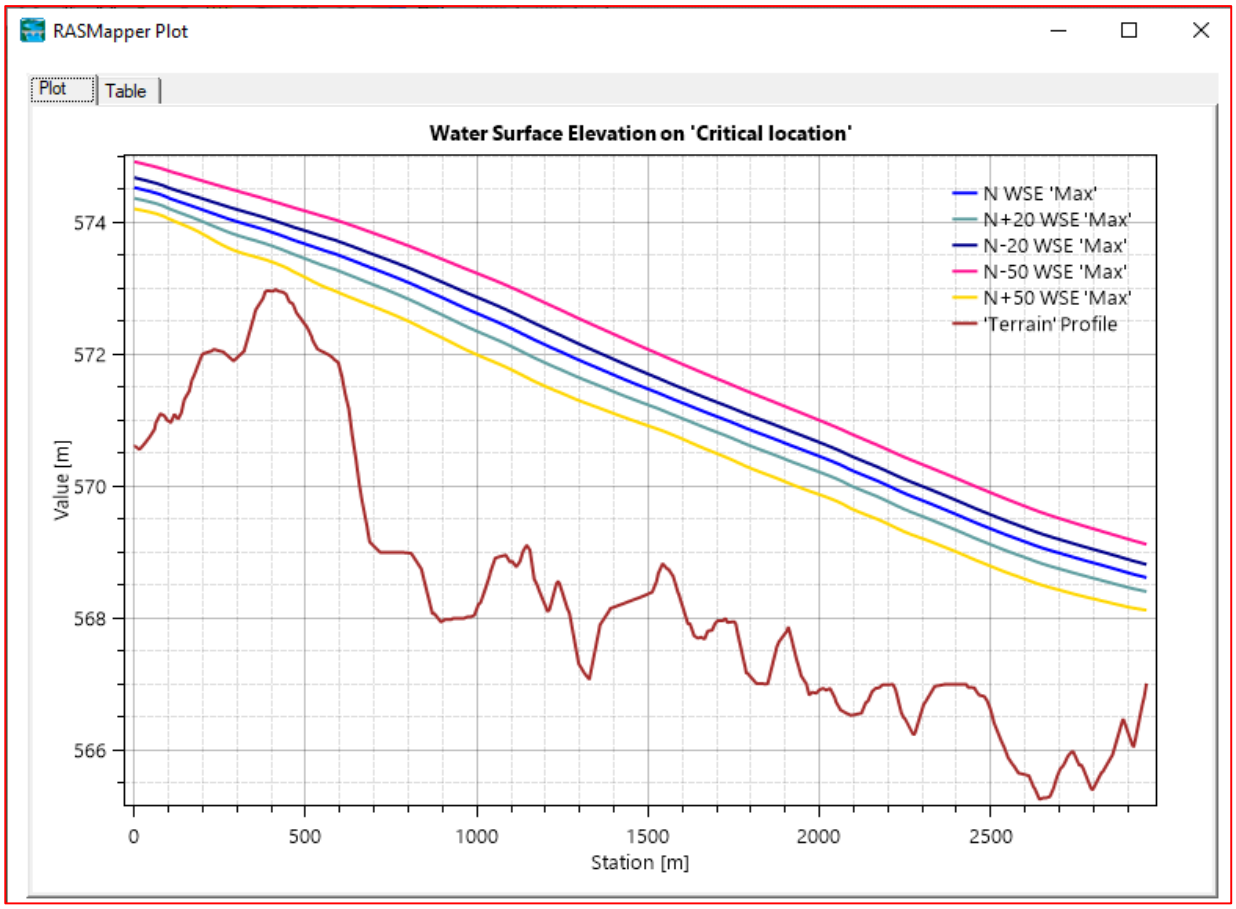

Figure 4.6: Sensitivity of WSE to change of manning’s roughness

4.2.2. Sensitivity of flood velocity to change of manning’s roughness at critical location

The sensitivity analysis conducted on the velocity values at a critical location reveals significant insights regarding the impact of Manning's roughness coefficient on hydraulic modeling. As shown on figure 4.7 below, as the roughness coefficient increases, a corresponding decrease in velocity is observed, and conversely, a decrease in the roughness coefficient leads to an increase in velocity. This relationship indicates that the flow dynamics are highly sensitive to variations in the roughness parameter, which is crucial for the accuracy of flood velocity simulations. By understanding this sensitivity, researchers can better gauge how fluctuations in the roughness coefficient affect model outputs, ultimately enhancing the reliability of flood predictions. Such analyses are essential for refining hydraulic models, as they inform practitioners about the potential variability in flood behavior under different conditions. This knowledge is particularly valuable for flood risk management, enabling more informed decisions in environmental planning and infrastructure design. Consequently, the findings from this sensitivity analysis not only contribute to the accuracy of hydraulic models but also improve our understanding of the river system's behavior in response to various flow scenarios, thus facilitating better preparedness for flood events.

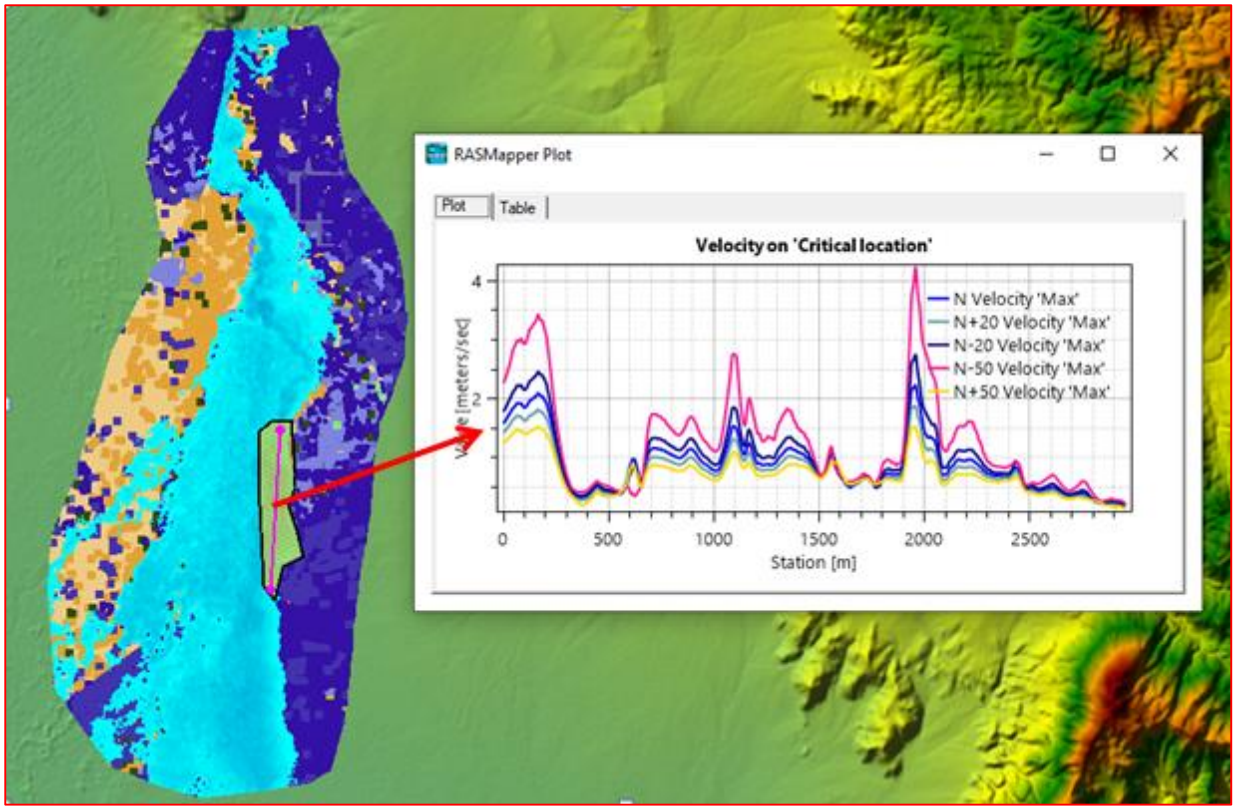

Figure 4.7: Sensitivity of flood velocity to change of manning's roughness

4.3.HEC-RAS Model calibration

Figure 4.8 below, presents the results of the simulated WSE values obtained after conducting a sensitivity analysis of Manning's roughness for the floodplain of the Weito River. Specifically, the figure shows the comparison between the simulated WSE values and the observed (measured) WSE values. Based on the description provided, it appears that the simulation results using the Manning's roughness coefficient adjusted during calibration (N) yielded a good fit to the measured WSE values. This suggests that the chosen value of Manning's roughness coefficient accurately captured the flow characteristics and resulted in simulated WSE values that align closely with the observed data.

By successfully calibrating the model and obtaining a good fit between the simulated and observed WSE values, the accuracy and reliability of the hydraulic model for the Weito River floodplain are improved. This calibrated model can then be used for various applications, such as flood risk assessment, hydraulic design, and scenario analysis, with increased confidence in the simulation results.

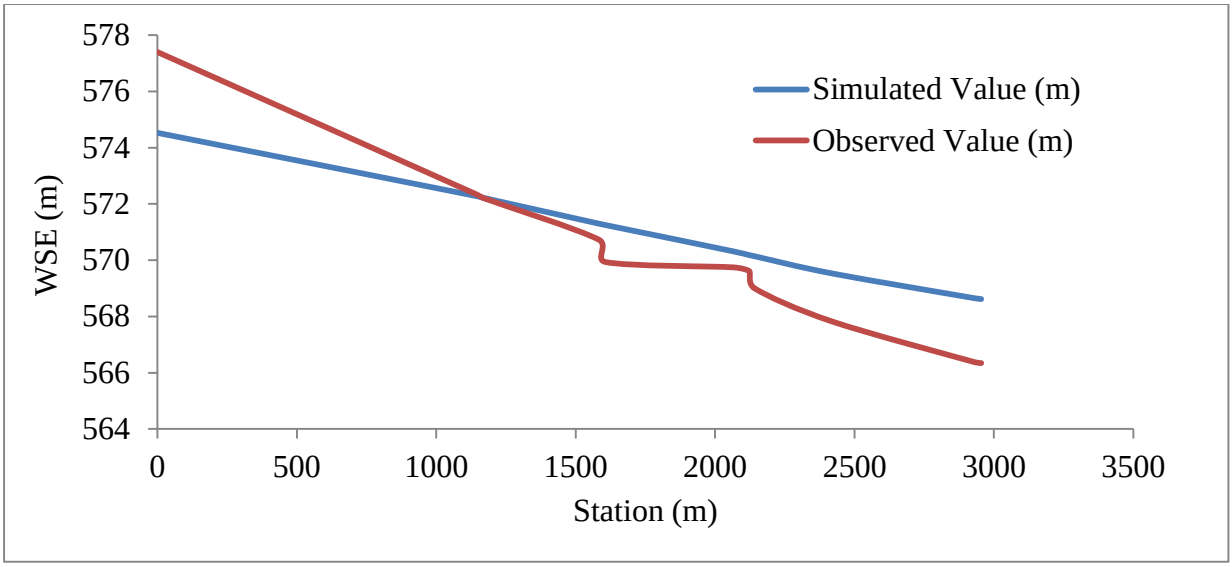

Figure 4.8: Calibrated result of WSE for manning's roughness N

4.4. Model evaluation

As shown on results presented in Figure 4.9 below, the coefficient of determination (R^2) is reported as 0.97. This indicates that the model performed very well in capturing the relationship between the simulated output and the observed values. With an R^2 value of 0.97, a large proportion (97%) of the variance in the measured data can be explained by the simulated values. Generally, higher values of R^2 indicate less error variance and a better fit between the simulated and observed data. R^2 values greater than 0.5 are often considered acceptable, indicating a reasonable level of accuracy in the model's performance. Therefore, an R^2 value of 0.97 suggests that the model has a strong ability to reproduce the observed parameters and is likely a reliable tool for predicting future data. However, the Nash-Sutcliffe Efficiency (NSE) value of 0.74, while still indicating acceptable predictive skill (NSE > 0.5), highlights limitations in the model's accuracy relative to the observed mean.

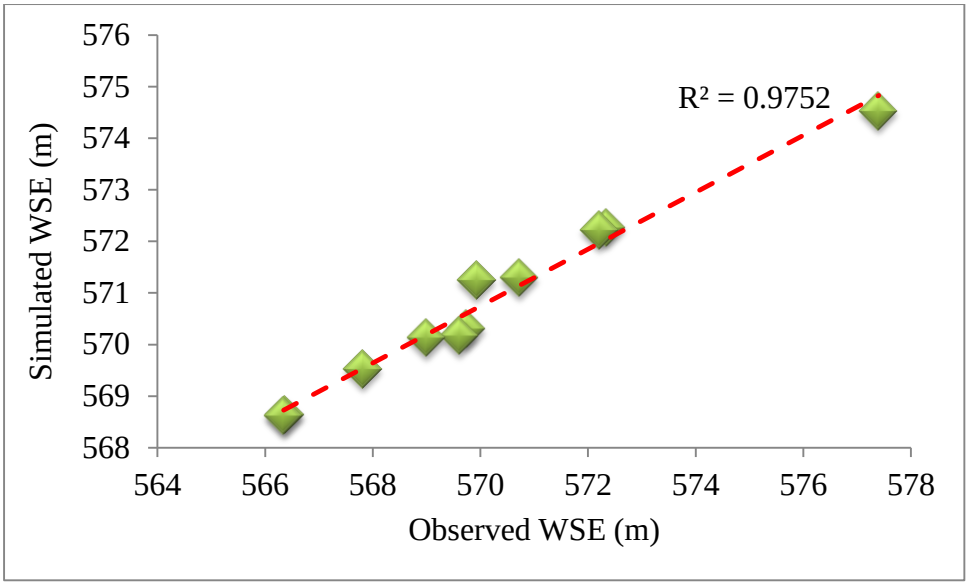

Figure 4.9: Goodness of fit for simulated and observed values of WSE

4.5.Flood extents map

Flood extent map is aimed to assess the flood inundation in the area by developing maps for different return periods. These maps help to identify flood-prone areas and establish flood-risk zones within those areas. These maps indicate the extent of flood inundation in the region for each return period. The total area affected by a 100-year flood was determined to be 2763.3 hectares. The flood inundation areas for the 50-year, 25-year, and 10-year return periods were determined to be 2497.7 hectares, 2239.4 hectares, and 1711.2 hectares, respectively. These figures indicate the potential extent of flooding for different magnitudes of floods and different return periods. Many rural areas downstream of Weito Bridge were prone to flooding. This suggests that the risk of floods extends beyond urban areas and affects a significant portion of the region. Figure 4.6 below likely illustrates the flood inundation extents of Lower Weito River on Rural settlements town downstream specifically for the 100-year return period.

Figure 4.10: Rural settlements under 100 years flood

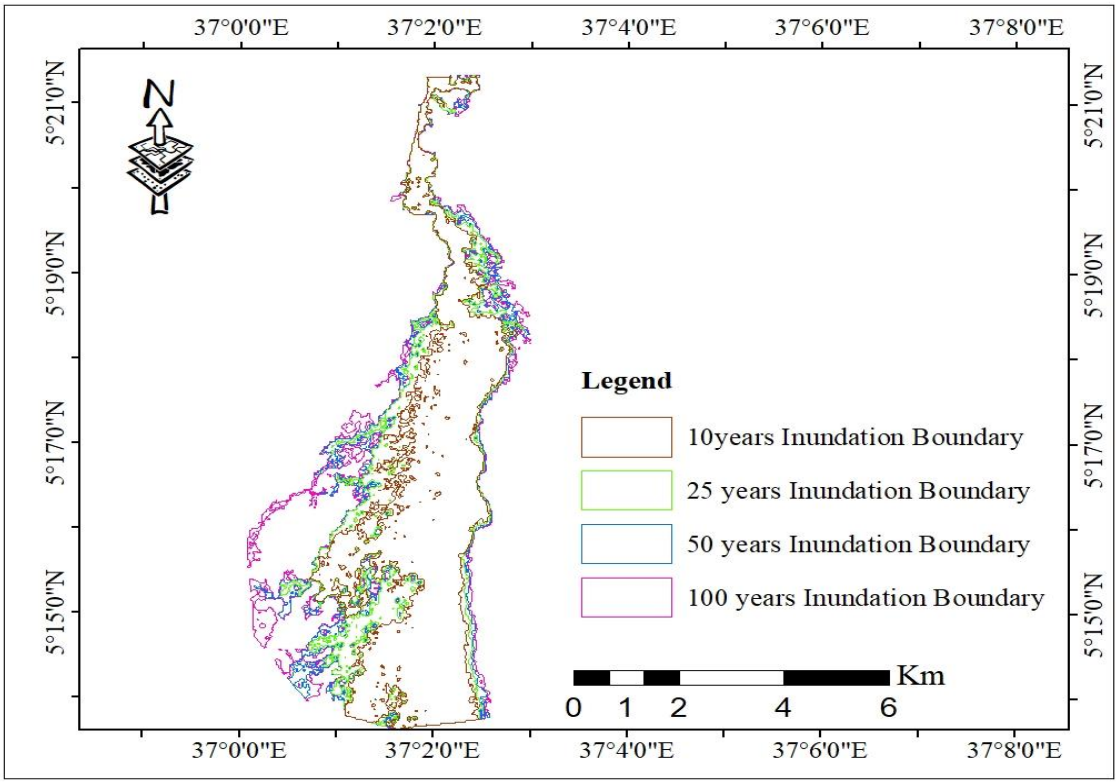

Figure 4.11: Flood inundation boundary for different return periods

4.6.Flood depth

In flood risk assessment and emergency response planning, understanding the extent and depth of inundation is crucial for emergency responders. The information provided in the study regarding the Lower Weito River flood depths for different return periods is valuable in this regard. The study indicates that for the 100-year flood event, the flood depth ranges from 0.001 meters (virtually low flooding) to a maximum of 7.5 meters. This wide range signifies the variability in flood depths within the flood-prone area. It is important to note that the maximum flood depth is found at the centerline of the river channel and gradually decreases along the cross section for all return periods. For the 10-year return period, the maximum flood depth is 6.56 meters, while for the 25-year and 50-year return periods; the maximum depths are 6.91 meters and 7.2 meters respectively. These values demonstrate the increasing severity of flooding with longer return periods. The gradual decrease in flood depth along the cross section indicates that the floodwaters spread out and lose energy as they move away from the river channel.

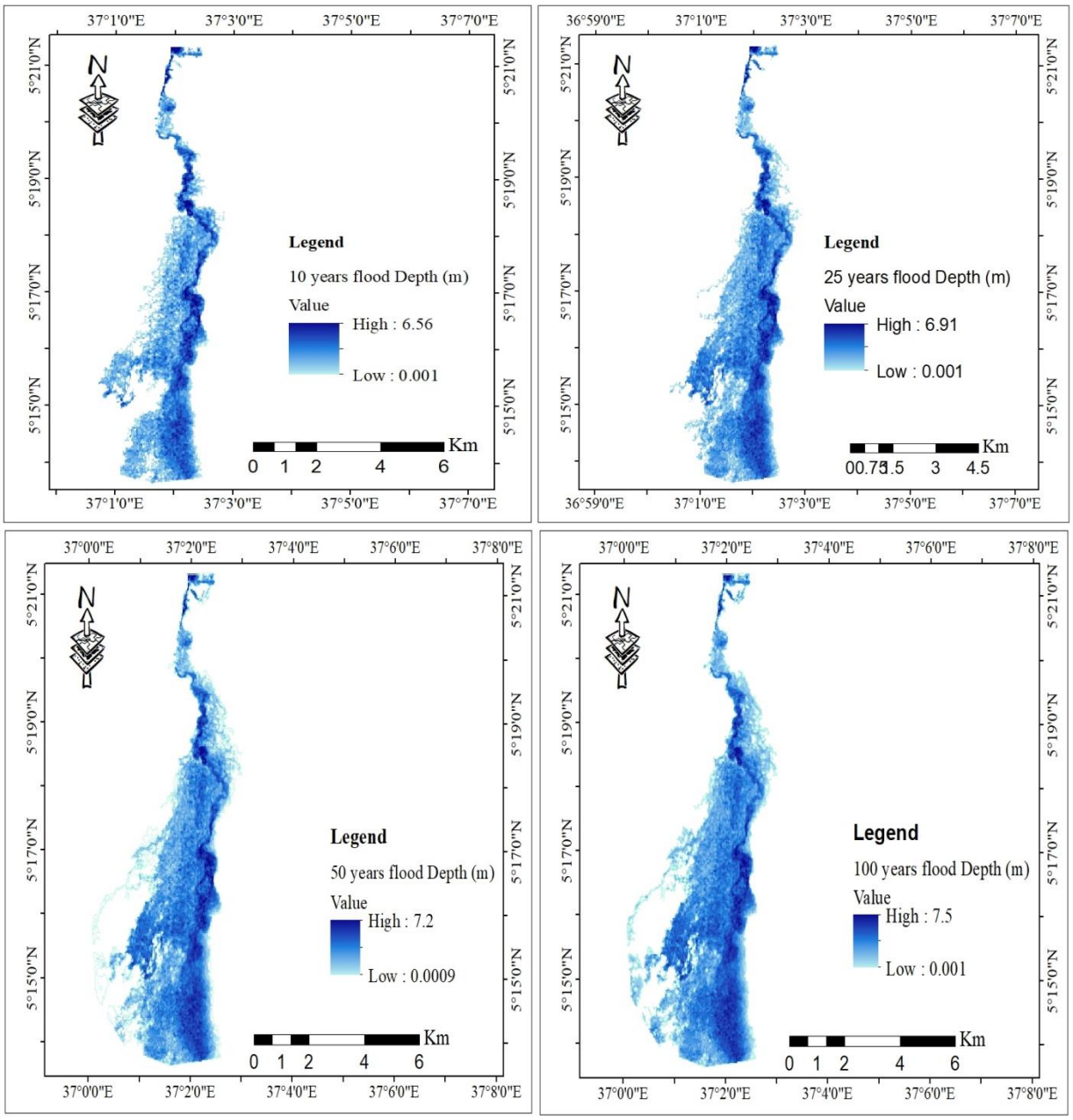

Figure 4.12: Flood depth for different return periods

4.7.Flood Velocity

The flood velocity map for the Lower Weito River provides important information about the spatial variation of flow velocities during flood events. The map shows the different flood velocities across the area, with each velocity range represented by a distinct color. In this case, the flood velocities range from a minimum velocity to a maximum velocity. The maximum flood velocities for different return periods are provided, indicating the highest velocities that can be expected during floods with specific recurrence intervals. For example, the maximum flood velocities for 10, 25, 50, and 100-year return periods are 3.15, 3.42, 3.67, and 7.02 m/s respectively. The significance of flood velocities lies in their potential impact on structures and the ability to implement emergency measures. It is generally accepted that higher flow velocities increase the likelihood of structural damage. When floodwater flows at high velocities, it limits the available time for implementing emergency measures such as using mobile protection elements (e.g., sandbags) or conducting evacuations.

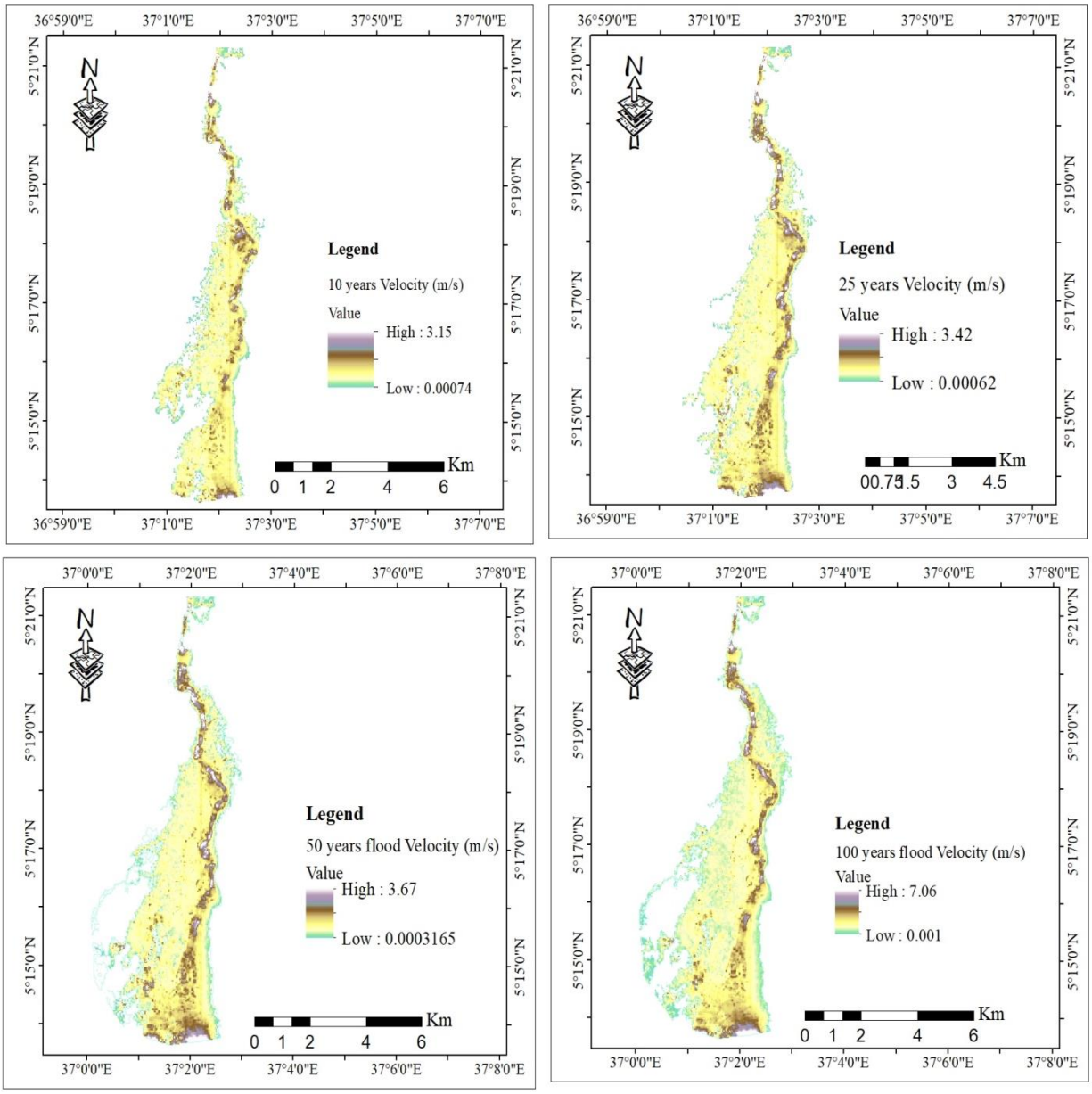

Figure 4.13: Flood velocities for different return periods

4.8.Flood hazard mapping

Lower Weito river flood hazard classification was prepared by considering the combined effect of flood depth and velocity based on FEMA (2018) hazard classification criteria. These hazard criteria were assigned hazard index on 1 – 5 scale, 1 being low hazard category while 5 being extreme hazard category. The hazard classification scheme developed by FEMA (2018) is shown in table 4.3 below.

Table 4.3: Flood Depth and Velocity Severity Grid Categories source: **(FEMA, 2018)**

Flood	Flood severity	Depth *velocity	Description

index	category	range (m^2 /sec)	
1	Low hazard	$\leq$ 0.2	Generally safe for vehicles, people and buildings.
2	Medium hazard	0.2 - 0.5	Unsafe for small vehicles.
3	High hazard	0.5 - 1.5	Unsafe for vehicles, children and elderly.
4	Very high hazard	1.5 - 2.5	Unsafe for vehicles and peoples
5	Extreme hazard	> 2.5	Unsafe for all vehicles, peoples, and buildings

Using the maps of (Depth * Velocity) for 100 years return periods and using the hazard classification scheme mentioned in Table 4.4, the hazard map for 100 years return periods has been prepared and is shown in Figures 4.19 below. These maps are the backbone for preparation of emergency action plan in the short term and floodplain regulatory management in the long term.

Table 4.4: Hazard categories and area coverage

Hazard categories	Coverage percentage
Low	21%
Medium	35%
High	29%
Very high	14%
Extreme	1%

As indicated on table above, about 21 % of the total flooded area is under low hazard. This category indicates areas that are relatively safe for vehicles, people, and buildings. While there may be some flooding, the hazard is considered low, and these areas are generally manageable and pose minimal threats. 35 % of the total flooded area is under medium hazard which is unsafe for small vehicles. This suggests that the water levels are higher, making it challenging for smaller vehicles to navigate through the flooded areas. However, it may still be relatively safe for people and buildings. About 29% of the total flooded area is under high hazard which is Unsafe for vehicles, children and elderly. This category denotes areas that are unsafe for vehicles, children, and the elderly. The higher water levels and velocity pose a significant risk to vehicles and may make evacuation or movement difficult. Additionally, it highlights the potential danger for vulnerable populations such as children and the elderly, who may have

difficulty navigating or evacuating during flooding events. 14% of the total flooded area is under very high hazard of flooding. Areas falling into this category pose a very high risk of flooding. They are considered unsafe for vehicles and people. The severity of the flooding is such that even vehicles may struggle to navigate through these areas, and people face significant risks to their safety. Precautions and evacuation measures are crucial in these zones. About 1 % of the total flooded area is under an extreme hazard of flooding which means unsafe for all peoples, vehicles and structures vulnerable to flooding. This classification represents the most severe and dangerous flooding conditions. Areas categorized as extreme hazard are highly unsafe for all individuals, vehicles, and structures vulnerable to flooding. The risk to life and property is extremely high, and these areas require immediate evacuation and extensive flood management measures. figure

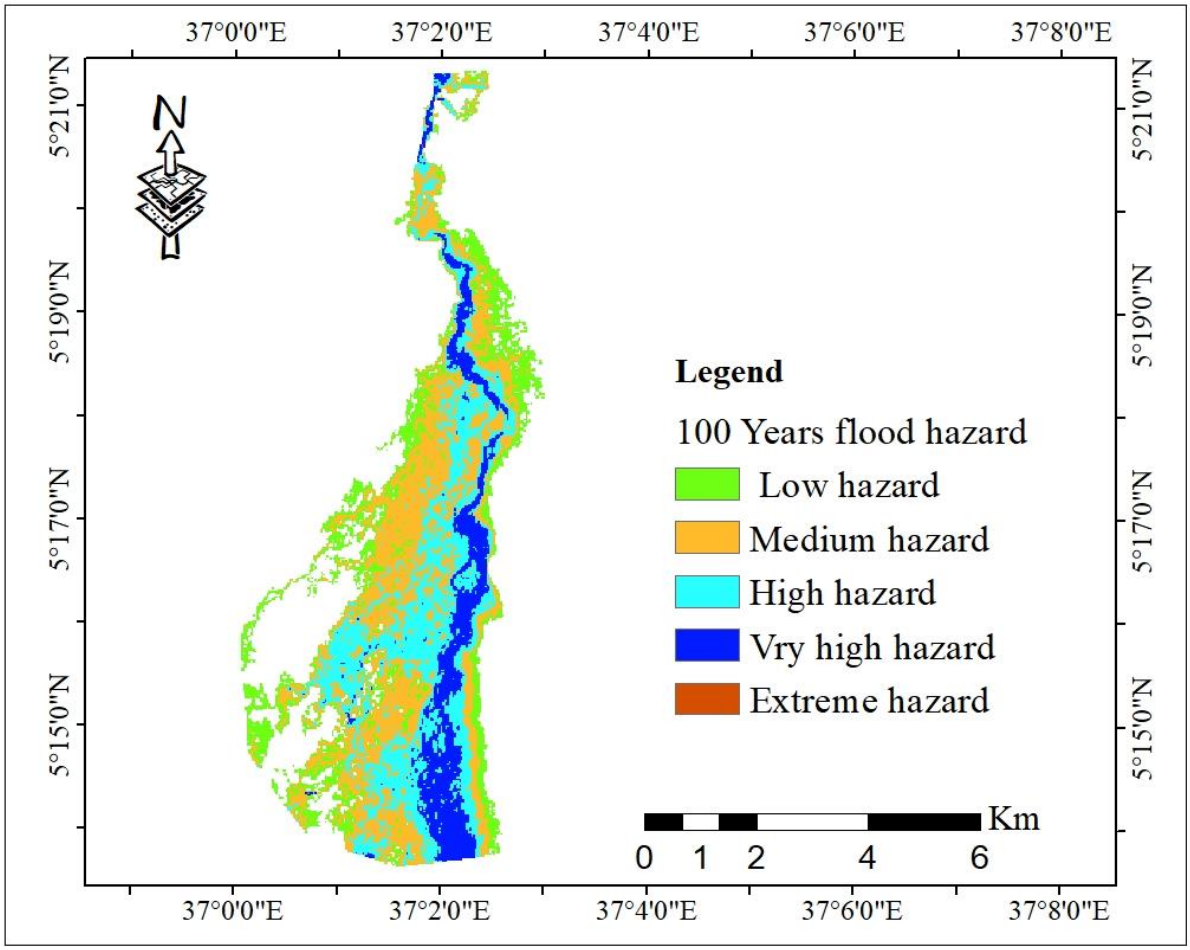

Figure 4.14: Flood hazard mapping

Generally, the hazard map provide valuable insights into the potential impacts of flooding, taking into account both the depth of water and the velocity of the floodwaters. The study

highlights the relationship between these factors and the associated risks to life and infrastructure.

It is well known that as the depth of water increases, the potential for damage also increases. This is because higher water depths exert greater pressure on structures, increasing the likelihood of structural failure or damage. The study emphasizes the importance of considering the depth of water in assessing flood hazards, as it directly correlates with the potential for damage to buildings and their foundations. Furthermore, the study emphasizes the critical role of floodwater velocity in determining the risk to human life. It highlights that faster-moving floodwaters pose a higher chance of loss of life. This is because swift currents can easily overpower individuals, making it difficult for them to escape or stay afloat. The study underscores the need to prioritize safety and evacuation measures when dealing with high-velocity floodwaters.

Even small depths of water moving at high velocities can be hazardous to structures and their foundations.

4.9.Flood Vulnerability Map

The vulnerability assessment conducted in the study provides a comprehensive understanding of the flood vulnerability across the study area. The vulnerability classes identified in the analysis were range from very low to very high, representing varying levels of susceptibility to the impacts of flooding. According to the results presented in the table 4.5 and Figure 4.20, it is observed that approximately 44% of the flooded area, equivalent to 1109.3 hectares, falls under the high and very high vulnerability classes. This portion of the flooded area is predominantly comprised of urban areas within rural settlements town and areas with medium-density rural populations located within the flood zone. The high and very high vulnerability classification suggests that these areas are more prone to the adverse impacts of flooding, indicating a greater risk to human life, infrastructure, and economic activities.

On the other hand, the majority of the study area, encompassing 56% of the total area, is categorized under medium to low vulnerability classes. This implies that these regions are relatively less vulnerable to flooding compared to the high and very high vulnerability areas. The medium vulnerability areas may still experience significant impacts from flooding, but they are not as severely exposed as the high vulnerability areas. The low vulnerability areas are even less susceptible to flood-related risks, indicating a lower likelihood of adverse consequences.

Furthermore, the study found that a substantial portion of the study area, which constitutes the remaining percentage of the flooded area, is classified under the very low vulnerability class. This classification suggests that these areas have a minimal susceptibility to the impacts of flooding. These regions are relatively safe and less likely to experience significant damage or adverse effects during flood events.

By providing a detailed vulnerability assessment, the study enables decision-makers, urban planners, and emergency management authorities to identify and prioritize areas that require immediate attention and mitigation measures. The focus can be directed towards the high and very high vulnerability areas, where interventions such as infrastructure improvements, flood mitigation measures, and emergency response planning can be implemented to reduce the risks and enhance resilience.

Conversely, the results also highlight areas with lower vulnerability, indicating relatively safer regions. These areas can serve as potential resettlement zones or areas for future development, considering their lower susceptibility to flooding.

Table 4.5: Flood vulnerability level and coverage

Vulnerability Level	Areal coverage (ha)	Percentage coverage
Very low	350.6	14%
Low	578.02	23%
Moderate	493.49	19%
High	424.9	17%
Very high	684.4	27%

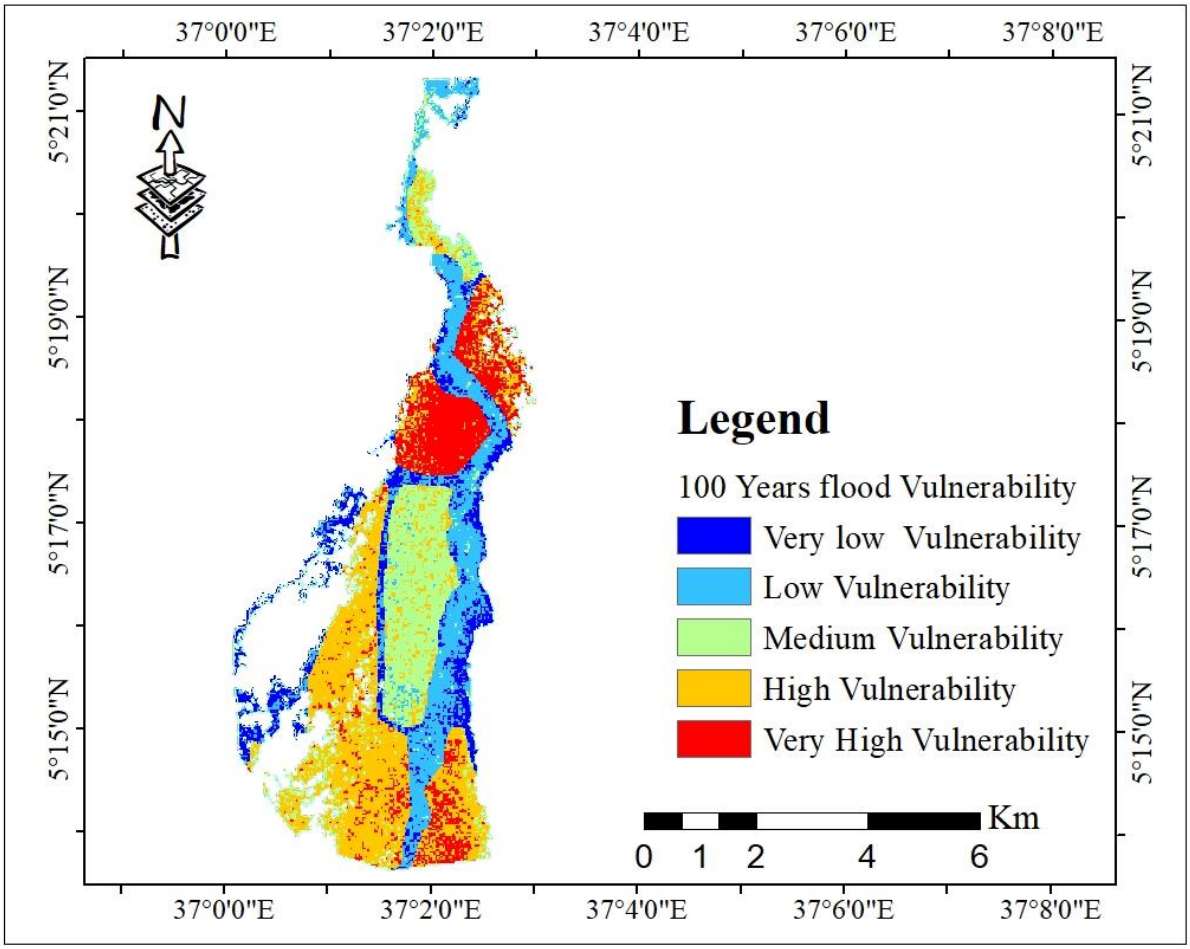

Figure 4.15: Lower Weito river Flood vulnerability map

4.10. Flood Risk Map

The flood risk assessment conducted in the study takes into account two key factors: hazard and vulnerability. By combining these factors, the study presents a comprehensive understanding of the flood risk along the Lower Weito River. Figure 4.21 provides an overview of the flood risk levels, which are categorized into five levels ranging from very low to very high risk. These risk levels indicate the potential consequences of flooding in different areas and provide insight into the severity and likelihood of damage to life, infrastructure, and economic activities. According to the results, approximately 62% of the flooded areas are classified as very high, high, and medium risk. These areas are particularly vulnerable to the adverse impacts of flooding, indicating a higher likelihood of significant damage and loss. The regions characterized by very high and high risk are primarily rural town settler's areas where substantial loss of life and infrastructure damage has been identified. These areas are densely populated and have a higher concentration of critical infrastructure. The medium-risk zones,

covering a portion of the flooded area, are characterized by scattered rural settlements with varying population densities, ranging from medium to low. These areas are vulnerable to flood-related risks, including damage to infrastructure and agricultural lands. While the level of risk is lower compared to the very high and high-risk areas, it still signifies the potential for significant impacts on communities and their livelihoods. On the other hand, approximately 38% of the flooded area falls under low and very low-risk categories. These areas are less susceptible to the adverse consequences of flooding, indicating a lower likelihood of significant damage or loss. The low-risk zones may include agricultural lands, sparsely populated areas, or regions with effective flood mitigation measures in place.

The results of the flood risk assessment are vital for decision-makers, urban planners, and emergency management authorities. They help prioritize interventions and resource allocation to areas with higher flood risk levels. The focus can be directed towards implementing measures such as improved infrastructure, early warning systems, land-use planning, and community awareness programs in the very high, high, and moderate-risk areas. This approach aims to reduce the vulnerability and enhance the resilience of these communities. Table 4.6 below shows the flood risk levels and coverage of Lower Weito River.

Table 4.6: Flood risk levels and coverage

Risk Level	Area (ha)	Percentage coverage
Very low	335.6	12.20%
Low	713.2	25.92%
Moderate	1270.6	46.17%
High	432.3	15.71%
Very high	0.25	0.01%

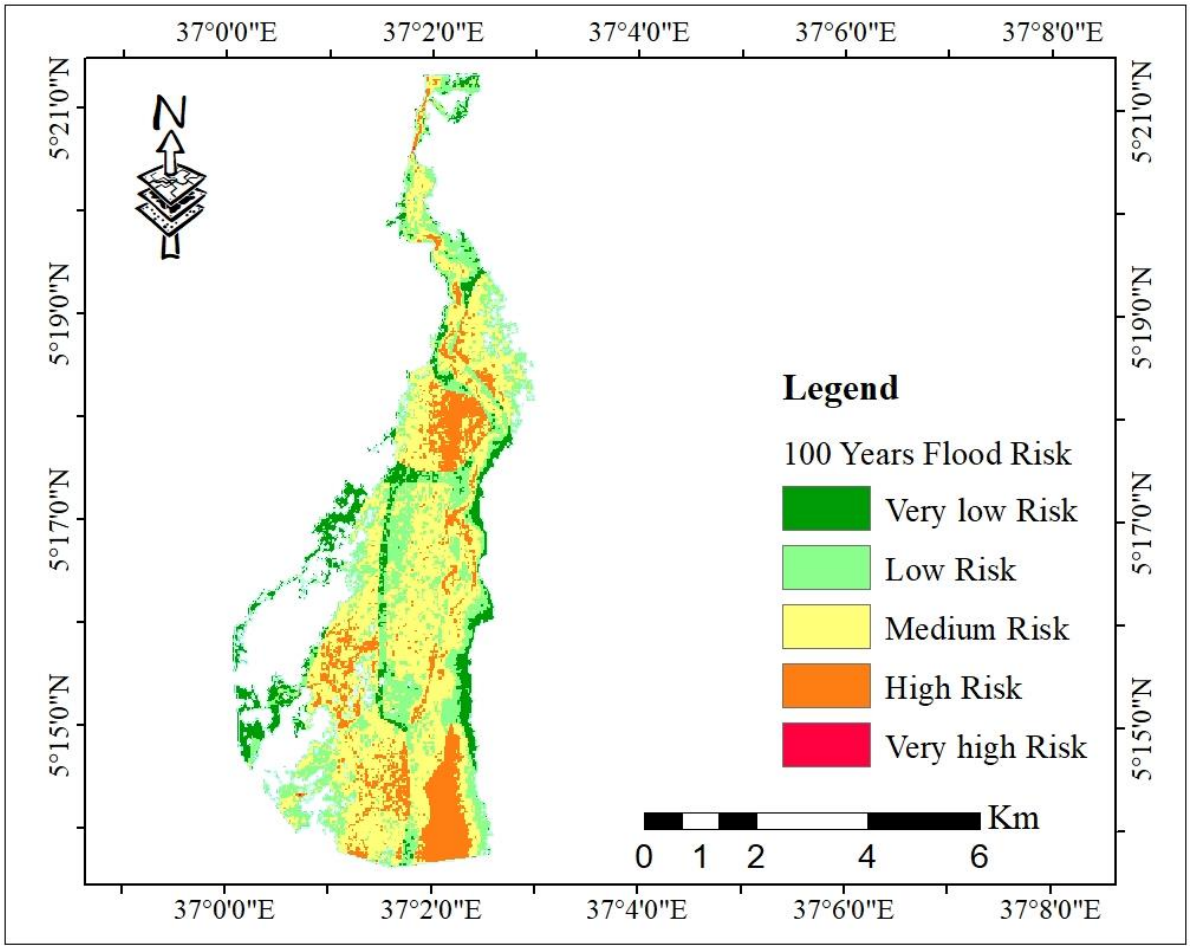

Figure 4.16: Flood risk map of Lower Weito River

.

5. CONCLUSIONS AND RECOMMENDATIONS

5.1.Conclusions

Floods occur whenever the capacity of the natural or manmade drainage system is unable to cope with the volume of water generated by rainfall. The current study was conducted on Lower Weito River which is the one of the tributary of Chew Behir Lake. The main objective of this study was to model and map the flood inundation and risk associated with the occurrence of flooding. In order to achieve the objectives of this study, existing Meteorological, hydrologic and topographic data collected from different organizations were used. These data are, meteorological data, stream flow data, manning's roughness coefficient of the site, topographic and land use/land cover data. The meteorological data has been collected from NMA, The flow data was collected from Hydrology Department of Ministry of Water and energy (MoWE), whereas the Geometric data was prepared from high resolution DEM 12.5m *12.5m which was downloaded from the Alaska Satellite Facility. The land use data used for flood vulnerability map was collected from field observation. The manning's roughness coefficient has been collected from field survey and has been verified from relevant literature Chow (1959).

The materials and tools used for study are: HEC HMS, HEC-RAS model, GIS software, GPS, Metering tape. In order to analyze the flood hazard and risk analysis, the inflow design flood for different return period was developed using HEC-HMS. Daily rainfall data were collected over a period of 1990- 2015 and Observed stream flow data were collected over a period of 1990-2007 available from MoWE was used Hydrologic flood frequency analysis in HEC HMS model. The model was calibrated and validated using actual stream flow data. In the current study, the model calibration was done by using the sensitive parameters to achieve a goodness of fit between simulated and observed data. The auto-calibration (through optimization trials) available in the HEC-HMS model was used for optimizing the model parameters. Observed daily rainfall and stream flow data from 01 January, 1990 to 31 December, 2001 were used in the calibration process. The calibration results shows there was strong relationship between simulated and observed stream flow data as the R2 as well as the NSE values were 0.82 and 0.77 respectively which was greater than 0.75 for the calibration period, and this indicates a high level of agreement between the simulated and observed data. R2 and NSE values approaching 1 indicate a better model and values closer to 0 consider a worse model. The

results obtained during the validation process at the Weito bridge station shows that R2 values of 0.78 and NSE of 0.75. These results can be judged as very good performance.

After model was calibrated and validated using actual observed flow data, the annual maximum precipitation of all years was extracted from the available rainfall data to develop the frequency storm for different return periods which later used as an input for HEC-HMS model to develop flood hydrograph for different return periods. To develop flood inundation, flood hazard, flood vulnerability and flood risk map of an area, HEC-RAS model was used. The result indicated that, the areas inundated by floods are 1711.2 ha, 2239.4 ha, 2497.7 ha, and 2763.3 ha for 10, 25, 50, and 100, years return periods respectively. The results of flood depth and velocity shows that, the maximum flood depth of 6.56, 6.91, 7.2, and 7.5 m and maximum flood velocities 3.15, 3.42, 3.67, and 7.01 m/s for return periods of 10, 25, 50, and 100 years respectively. To identify the potential danger or hazard associated with the flood, flood hazard maps were derived taking into account the depth and velocity and duration of the floodwaters. Flood hazard map for 100 year return periods has been prepared and the result shows that about 0.01% of the total flooded area is under an extreme hazard, 14% of the total flooded area is under very high hazard whereas 29%, 35% and 21% of total area are under high, medium and low hazard respectively. The result indicated that almost 43% of the flooded area is under extreme, very high hazard and high hazard. This map is used to identify areas at risk of flooding, and consequently to improve flood risk management and disaster preparedness.

The flood vulnerability map of the area was prepared by considering the vulnerability indicators such as flood depth, flood velocity, flood duration, slope, land use land cover, and DEM. The flood vulnerability is classified to five areas of vulnerability classes ranging from very low to very high. About 44% of flooded area is under high and very high vulnerability, 19% of an area is covered with moderate vulnerability class and 37% of an area is covered with low and very low vulnerability classes. The flood risk map of an area was prepared by considering flood hazard and flood vulnerability. The flood risk is divided into five levels of risk ranging from very low to very high risk. The result shows that Very high and high risk covers 16%. The medium risk class covers about 46% of the area while the low and very low flood risk zones constitute 38% of the area.

5.2.Recommendations

Based on the findings of this research the following recommendations can be drawn. Given the specific flood depths and velocities identified for different return periods, it is recommended to implement flood control measures in the areas most prone to flooding. This may include constructing flood embankments, levees, or floodwalls to minimize the extent and impact of flooding. Additionally, implementing erosion control measures along the riverbanks can help reduce the risk of bank erosion during flood events. The flood vulnerability map generated in the study identified areas with varying levels of vulnerability. It is recommended to incorporate this information into land use planning processes. Restricting or regulating development in high and very high vulnerability areas can help mitigate flood risks. This can be achieved through zoning regulations, building codes, and enforcing setbacks from flood-prone areas. With the knowledge of flood depths, velocities, and return periods, it is crucial to establish and enhance early warning systems in the Lower Weito River area. This can involve the installation of river level monitoring stations, rainfall gauges, and the development of a robust communication network to disseminate timely flood warnings to at-risk communities. Public education and awareness campaigns should accompany the early warning systems to ensure that residents understand the warnings and know how to respond. Based on the flood hazard and risk maps, it is essential to strengthen emergency preparedness and response mechanisms in the Lower Weito River area. This includes developing and regularly updating comprehensive flood emergency response plans, conducting drills and exercises to test preparedness, and establishing evacuation routes and shelters in high-risk areas. Collaborating with relevant stakeholders such as local authorities, emergency services, and community organizations is vital for effective flood response.

Future studies should explore the effectiveness of integrated flood management approaches those combine hydrological modeling with community engagement. Research could focus on successful case studies from other regions that have implemented similar strategies to inform local practices. While this study utilized historical meteorological data, future research should aim to establish a continuous monitoring network for real-time data collection. Investigating the impacts of climate change on rainfall intensity and frequency over time would provide valuable insights into evolving flood risk. This study primarily relied on HEC-HMS and HEC-RAS models. Future research could investigate the application of alternative modeling frameworks, such as MIKE 21 or J2000, and incorporate machine learning techniques for

improved calibration and validation in diverse hydrological conditions. Although some community engagement was addressed, future studies could assess the effectiveness of targeted public awareness campaigns on flood preparedness. Research could explore the role of social media and local workshops in enhancing community resilience. The study identified flood risk areas, but did not explore the socio-economic implications in detail. Future research should conduct comprehensive assessments of the economic impacts of flooding on livelihoods, property values, and local businesses. While infrastructure improvements were recommended, future studies could analyze the current state of flood defenses and drainage systems. Research could include risk assessments of critical infrastructure to identify vulnerabilities under extreme weather events. The flood vulnerability map developed in this study should be further refined. Future research could incorporate factors such as community demographics, economic status, and historical flooding trends to create more nuanced vulnerability assessments. Future research should explore specific climate adaptation measures, such as green infrastructure solutions, and evaluate their effectiveness in flood mitigation. Studies could also investigate the potential for community-led initiatives in enhancing local resilience.

6. REFERENCES

Adeboye, O. B., & Alatise, M. O. (2007). Performance of Probability Distributions and Plotting Positions in Estimating the Flood of River Osun at Apoje Sub-basin, Nigeria. *E-Journal - Internationale Kommission Für Agrartechnik*, *IX*, 1–21.

Adeyi, G., Ibraheem, A., & Onyeocha, N. (2020). *Unit Hydrograph: Concepts, Estimation Methods and Applications in Hydrological Sciences*.

Adigrat, M., Region, T., Nigusse, A. G., & Adhanom, O. G. (2019). *Flood Hazard and Flood Risk Vulnerability Mapping Using Geo-Spatial and*. *11*(1), 90–107.

Ahmad, S., Khan, I. H., & Parida, B. P. (2001). *Performance of Stochastic Approaches for Forecasting River Water Quality | Request PDF*. https://www.researchgate.net/publication/11594832_Performance_of_Stochastic_Approaches_for_Forecasting_River_Water_Quality

Al, P. M. et. (2004). *Reducing disaster risk a challenge for development. United Nations Development Programme—Bureau for Crisis Prevention and Recovery. Doi:10.1007/ s003450050172*.

Alexander, D. E. (1997). The study of natural disasters, 1977-1997: Some reflection on a changing field of knowledge. *Disasters*, *21 4*, 284–304.

Anees, M. T., Abdullah, K., Nawawi, M. N. M., Ab Rahman, N. N. N., Piah, Abd. R. Mt., Zakaria, N. A., Syakir, M. I., & Mohd. Omar, A. K. (2016). Numerical modeling techniques for flood analysis. *Journal of African Earth Sciences*, *124*, 478–486. https://doi.org/10.1016/j.jafrearsci.2016.10.001

A.O., O., & Njogu, A. K. (2020). Using Extreme Value Theory to Estimate Available Water in the Upper Awach-Kibuon Catchment in Nyamira County, Kenya. *American Journal of Water Resources*, *8*(4), 200–210. https://doi.org/10.12691/ajwr-8-4-6

Awal, R., & Shakya, N. M. (2007). *Floodplain Analysis and Risk Assessment of Lakhandei River*.

Bahramifar, A., Shirkhani, R., & Mohammadi, M. (2013). *An ANFIS-based Approach for Predicting the Manning Roughness Coefficient in Alluvial Channels at the Bank-full Stage*. *26*(2), 177–186. https://doi.org/10.5829/idosi.ije.2013.26.02b.08

Beven, K. (2006). *Rainfall-Runoff Modeling: Introduction | Request PDF*. https://www.researchgate.net/publication/229703907_Rainfall-Runoff_Modeling_Introduction

Beven, K., & Binley, A. (1992). The future of distributed models: Model calibration and uncertainty prediction. *Hydrological Processes*, *6*(3), 279–298.

Birkmann, J. (2007). Risk and vulnerability indicators at different scales: Applicability, usefulness and policy implications. *Environmental Hazards*, *7*(1), 20–31. https://doi.org/10.1016/j.envhaz.2007.04.002

Busby, J. (2017). *Water Diplomacy As Possible Driver of Stability | PDF | Nile | Unrest*. https://www.scribd.com/document/471857325/Water-Diplomacy-as-possible-driver-of-stability

Chow, V. T. (1988). *Chow, V.T., Maidment, D.R. and Mays, L.W. (1988) Applied Hydrology. International Edition, McGraw-Hill Book Company, New York. - References—Scientific Research Publishing*. https://www.scirp.org/reference/referencespapers?referenceid=1165939

Cunderlik, J. M., & Simonovic, S. P. (2007). Hydrologic Models for Inverse Climate Change Impact Modeling. *18th Canadian Hydrotechnical Conference, January 2007*, 1–9.

Demissie, M. (2008). *REGIONAL FLOOD FREQUENCY ANALYSIS FOR UPPER AWASH SUB- BASIN (UPSTREAM OF KOKA)*.

Dilley, M., Chen, R. S., Deichmann, U., Lerner-Lam, A., Arnold, M., Agwe, J., Buys, P., Kjekstad, O., Lyon, B., & Yetman, G. (2005). Natural disaster hotspots: A global risk analysis. *World Bank Disaster Risk Management Series*, *5*, 1–132. https://doi.org/10.1007/978-3-322-82113-3_1

El-Naqa, A., & Zeid, N. A. (1993). A Program of Frequency Analysis Using Gumbel's Method. *Groundwater*, *31*(6), 1021–1024. https://doi.org/10.1111/j.1745-6584.1993.tb00876.x

Ethiopia: Disaster Prevention and Preparedness Agency Vol.13 No.3 - Ethiopia | ReliefWeb. (2006, July 30). https://reliefweb.int/report/ethiopia/ethiopia-disaster-prevention-and-preparedness-agency-vol13-no3

Ethiopia: Floods - Emergency Plan of Action (EPoA) DREF Operation n° MDRET023 - Ethiopia | ReliefWeb. (2020, September 27). https://reliefweb.int/report/ethiopia/ethiopia-floods-emergency-plan-action-epoa-dref-operation-n-mdret023

EU. (2022). *DIRECTIVE OF THE EUROPEAN PARLIAMENT AND OF THE COUNCIL*. *0344*.

Fahad, M. G. R., Nazari, R., Motamedi, M. H., & Karimi, M. E. (2020). Coupled hydrodynamic and geospatial model for assessing resiliency of coastal structures under extreme storm scenarios. *Water Resources Management*, *34*, 1123–1138.

Faulkner, D., & Wass, P. (2005). Flood estimation by continuous simulation in the Don catchment, South Yorkshire, UK. *Water and Environment Journal*, *19*(2), 78–84.

Feldman, A. (2000). *Hydrologic Modeling System HEC-HMS Technical Reference Manual. 157. - References—Scientific Research Publishing*. https://www.scirp.org/reference/referencespapers?referenceid=1675931

FEMA. (2018). *Guidance for Flood Risk Analysis and Mapping Flood Depth and Analysis Grids*. *February*.

Gebre, S. L. (2015). Application of the HEC-HMS Model for Runoff Simulation of Upper Blue Nile River Basin. *Journal of Waste Water Treatment & Analysis*, *06*(02). https://doi.org/10.4172/2157-7587.1000199

Gebre Sl, G. Y. (2015). Flood Hazard Assessment and Mapping of Flood Inundation Area of the Awash River Basin in Ethiopia using GIS and HEC-GeoRAS/HEC-RAS Model. *Journal of Civil & Environmental Engineering*, *05*(04). https://doi.org/10.4172/2165-784X.1000179

Gilley, J. E., Kottwitz, E. R., & Wieman, G. A. (1991). *Roughness Coefficients for Selected Residue Materials*.

Govindaraju, R. S., & Levent Kavvas, M. (1993). Development of an approximate model for unsaturated flow with root water uptake under rectangular water content profiles assumption. *Journal of Hydrology*, *146*, 321–339. https://doi.org/10.1016/0022-1694(93)90282-E

Grande, P. (2016). *Flood Hazard Identification Program Grande Prairie – Bear River – Flood Hazard Study – Summary*. 2016.

Haghighat, A. (2016). *Monte Carlo Methods for Particle Transport*. CRC Press. https://doi.org/10.1201/b17934

Horritt, M. S., & Bates, P. D. (2002). Evaluation of 1D and 2D Numerical Models for Predicting River Flood Inundation. *Journal of Hydrology*, *268*, 87–99. https://doi.org/10.1016/S0022-1694(02)00121-X

IPPC. (1995). *Scientific-Technical Analyses of Impacts, Adaptations, and Mitigation of Climate Change*.

Javadnejad, F., Waldron, B., & Hill, A. (2017). LITE Flood: Simple GIS-Based Mapping Approach for Real-Time Redelineation of Multifrequency Floods. *Natural Hazards Review*, *18*(3). https://doi.org/10.1061/(ASCE)NH.1527-6996.0000238

Jekel, H., Arle, J., Bartel, H., & Baumgarten, C. (2014). Water Resource Management in Germany. *Bundesministerium Für Umwelt, Naturschutz, Bau Und Reaktorsicherheit*, 150.

Khadka, A. (2014). *The Hydraulics of Open Channel Flow: An Introduction Basic principles, sediment motion, hydraulic modelling, design of hydraulic structures Second Edition*. https://www.academia.edu/40990022/The_Hydraulics_of_Open_Channel_Flow_An_Introduction_Basic_principles_sediment_motion_hydraulic_modelling_design_of_hydraulic_structures_Second_Edition

Khaligni, S. (2015). *Integrated application of HEC-RAS and GIS and RS for flood risk assessment in Lighvan Chai River*. https://www.researchgate.net/publication/308368287_Integrated_application_of_HEC-RAS_and_GIS_and_RS_for_flood_risk_assessment_in_Lighvan_Chai_River

Khan, S. (2012). Vulnerability assessments and their planning implications: A case study of the Hutt Valley, New Zealand. *Natural Hazards*, *64*(2), 1587–1607. https://doi.org/10.1007/s11069-012-0327-x

Khan, S. I., Hong, Y., Wang, J., Yilmaz, K. K., Gourley, J. J., Adler, R. F., Brakenridge, G. R., Policelli, F., Habib, S., & Irwin, D. (2011). Satellite Remote Sensing and Hydrologic Modeling for Flood Inundation Mapping in Lake Victoria Basin: Implications for Hydrologic Prediction in Ungauged Basins. *IEEE Transactions on Geoscience and Remote Sensing*, *49*(1), 85–95. https://doi.org/10.1109/TGRS.2010.2057513

Khattak, M. S., Anwar, F., Saeed, T. U., Sharif, M., Sheraz, K., & Ahmed, A. (2016). Floodplain mapping using HEC-RAS and ArcGIS: a case study of Kabul River. *Arabian Journal for Science and Engineering*, *41*, 1375–1390.

Kumar, S., Jaswal, A., Pandey, A., & Sharma, N. (2017). *Literature Review of Dam Break Studies and Inundation Mapping Using Hydraulic Models and GIS*. *04*(05).

Miranda, F. N., & Ferreira, T. M. (2019). A simplified approach for flood vulnerability assessment of historic sites. *Natural Hazards*, *96*(2), 713–730. https://doi.org/10.1007/s11069-018-03565-1

Nasiri, H., Johari, M., Yusof, M., Ahmad, T., & Ali, M. (2016a). An overview to flood vulnerability assessment methods. *Sustainable Water Resources Management*, *2*(3), 331–336. https://doi.org/10.1007/s40899-016-0051-x

Nasiri, H., Johari, M., Yusof, M., Ahmad, T., & Ali, M. (2016b). An overview to flood vulnerability assessment methods. *Sustainable Water Resources Management*, *2*(3), 331–336. https://doi.org/10.1007/s40899-016-0051-x

Ndue, K., & Baylie, M. M. (2023). *Determinants of Rural Households ' Intensity of Flood Adaptation in the Fogera Rice Plain , Ethiopia: Evidence from Generalised Poisson Regression*.

Neelz, S., & Pender, G. (2010). *Benchmarking of 2D hydraulic modelling packages*.

Nquot, I., & Kulatunga, U. (2014). Flood Mitigation Measures in the United Kingdom. *Procedia Economics and Finance*, *18*(September), 81–87. https://doi.org/10.1016/S2212-5671(14)00916-2

Pandey, A. C., Singh, S. K., Gyan, S., Univeristy, V., & Nathawat, M. S. (2010). *Waterlogging and flood hazards vulnerability and risk assessment in Indo Gangetic plain Waterlogging and flood hazards vulnerability and risk*. *June 2018*. https://doi.org/10.1007/s11069-010-9525-6

Pasche, E. (2008). *(Effectiveness and Efficiency of Non-structural Flood Risk Management Measures* |. https://www.researchgate.net/publication/281355131_Effectiveness_and_Efficiency_of_Non-structural_Flood_Risk_Management_Measures

Phien, H. N. (2001). Reservoir sedimentation with correlated inflows. *Journal of Hydrology*, *53*(3), 327–341. https://doi.org/10.1016/0022-1694(81)90009-3

Pramanik, N., Panda, R. K., & Sen, D. (2010). One Dimensional Hydrodynamic Modeling of River Flow Using DEM Extracted River Cross-sections. *Water Resources Management*, *24*(5), 835–852. https://doi.org/10.1007/s11269-009-9474-6

Rameshwaran, P., & Shiono, K. (2007). Quasi two-dimensional model for straight overbank flows through emergent. *Journal of Hydraulic Research*, *45*(3), 302–315. https://doi.org/10.1080/00221686.2007.9521765

Randa, T., Tom, R. O., George, K. O., Joanes, A. O., & Haron, A. (2022). Review of flood modelling and models in developing cities and informal settlements: A case of Nairobi city Journal of Hydrology: Regional Studies Review of flood modelling and models in developing cities and informal settlements: A case of Nairobi city. *Journal of Hydrology: Regional Studies*, *43*(October), 101188. https://doi.org/10.1016/j.ejrh.2022.101188

Roy, S., Atolagbe, B., Ghasemi, A., & Bathi, J. (2020). A MATLAB-Based Grid Generation Tool for Hydrodynamic Modeling. *Watershed Management Conference 2020*, 88–98.

Safaripour, M., Monavari, M., Zare, M., Abedi, Z., & Gharagozlou, A. (2012). Flood risk assessment using GIS (case study: Golestan province, Iran). *Polish Journal of Environmental Studies*, *21*(6), 1817–1824.

Saleh, F., Ducharne, A., Flipo, N., Oudin, L., & Ledoux, E. (2013). Impact of river bed morphology on discharge and water levels simulated by a 1D Saint–Venant hydraulic

model at regional scale. *Journal of Hydrology*, *476*, 169–177. https://doi.org/10.1016/j.jhydrol.2012.10.027

Sensitivity of Roughness Coefficient in Flood Modelling | LinkedIn. (n.d.). Retrieved April 16, 2025, from https://www.linkedin.com/pulse/sensitivity-roughness-coefficient-flood-modelling-gudagudi-gmice-a0fbe/

Serra-Llobet, A., Kondolf, george 'mathias, Schaefer, K., & Nicholson, S. (2018). Managing Flood Risk: Innovative Approaches from Big Floodplain Rivers and Urban Streams. In *Managing Flood Risk: Innovative Approaches from Big Floodplain Rivers and Urban Streams*. https://doi.org/10.1007/978-3-319-71673-2

Smit, B. (2006). *Adaptation , adaptive capacity and vulnerability*. *16*, 282–292. https://doi.org/10.1016/j.gloenvcha.2006.03.008

Tan, B., Uk, V. M., Uk, M. P., & Germany, J. P. (2012). *Determinants of Risk: Exposure and Vulnerability Coordinating Lead Authors: Lead Authors: Review Editors: Contributing Authors :* 65–108.

Tansar, H., Babur, M., & Karnchanapaiboon, S. L. (2020). Flood inundation modeling and hazard assessment in Lower Ping River Basin using MIKE FLOOD. *Arabian Journal of Geosciences*, *13*, 1–16.

Tsakiris, G. (2007). Practical application of risk and hazard concepts in proactive planning. *European Water*, *19*(20), 47–56.

UNISDR. (2009). *Terminology on disaster risk reduction. Retrieved from The united nations office for disaster risk reduction*.

United States Army Corps of Engineers (USACE) Post-Hurricane Katrina Levee Surveys | InPort. (2005). https://www.fisheries.noaa.gov/inport/item/50054

UNU-EHS. (2006). *Vulnerability a conceptual and methodological review*.

Vojtek, M., & Vojtekov, J. (2016). *Flood hazard and fl ood risk assessment at the local spatial scale: A case study*. *7*(6), 1973–1992.

Whitney, H. B. M. and D. R. (1947). On a Test of Whether one of Two Random Variables is Stochastically Larger than the Other Author (s): H. B. Mann and D. R. Whitney Source: The Annals of Mathematical Statistics , Vol. 18 , No. 1 (Mar ., 1947), pp. 50-60 Published by: Institute. *The Annals of Mathematical Statistics*, *18*(1), 50–60.

Yerramilli, S. (2012). A Hybrid Approach of Integrating HEC-RAS and GIS Towards the Identification and Assessment of Flood Risk Vulnerability in the City of Jackson, MS. *American Journal of Geographic Information System*, *1*(1), 7–16.

Yusoff, I. M., Ujang, M. U., & Rahman, A. A. (2008). Volumetric Soft Geo-Objects for GIS Based Urban Runoff Modelling. *Advances towards 3D GIS*, 463–491.

Zakaria, Z., & Shabri, A. (2012). Regional frequency analysis of extreme rainfalls using Partial L-moments method. *Theoretical and Applied Climatology*, *113*. https://doi.org/10.1007/s00704-012-0763-2

7. APPENDIX

Appendix A: population density on inundation area

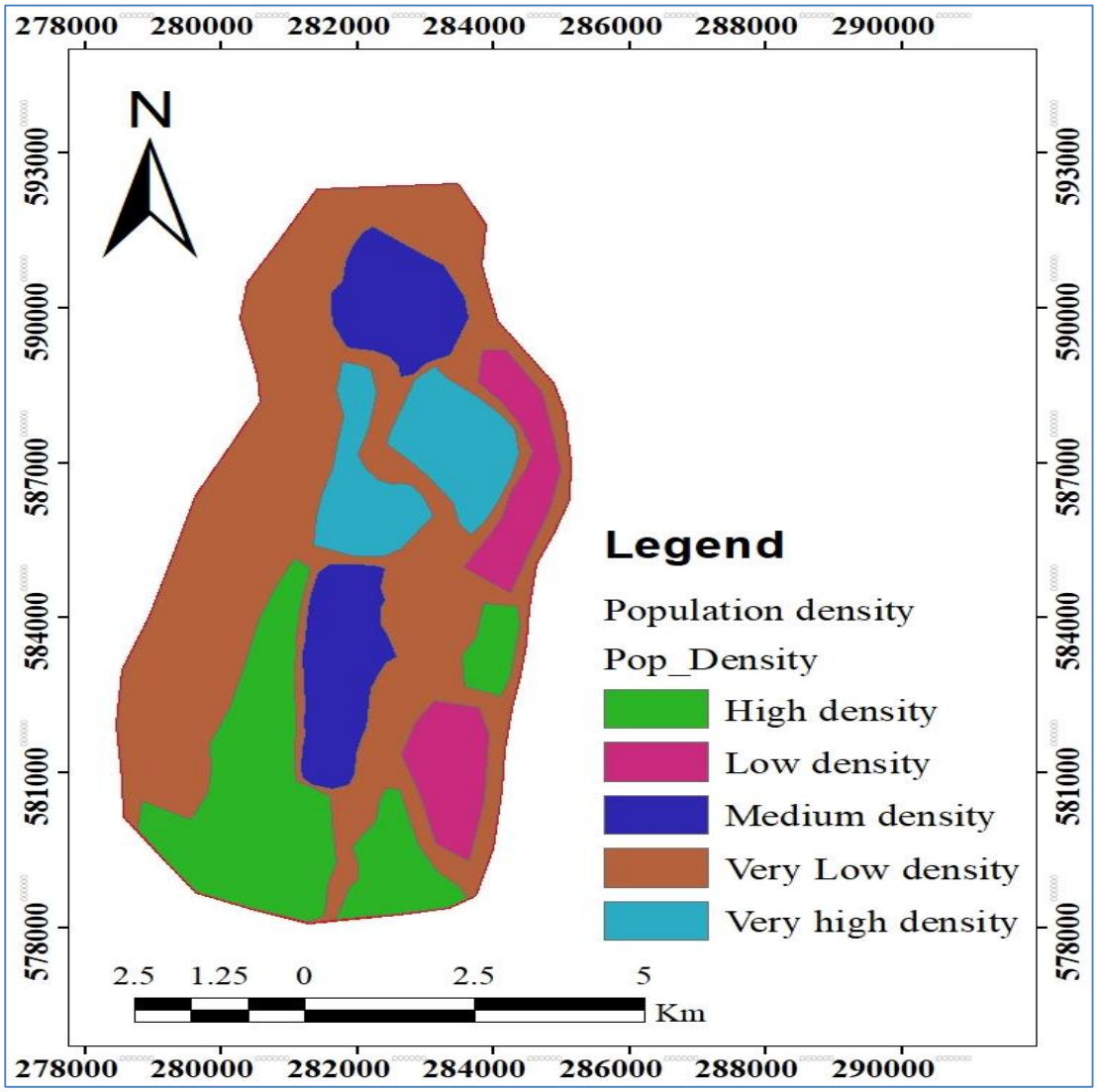

Appendix B: Slope of the terrain in inundation area

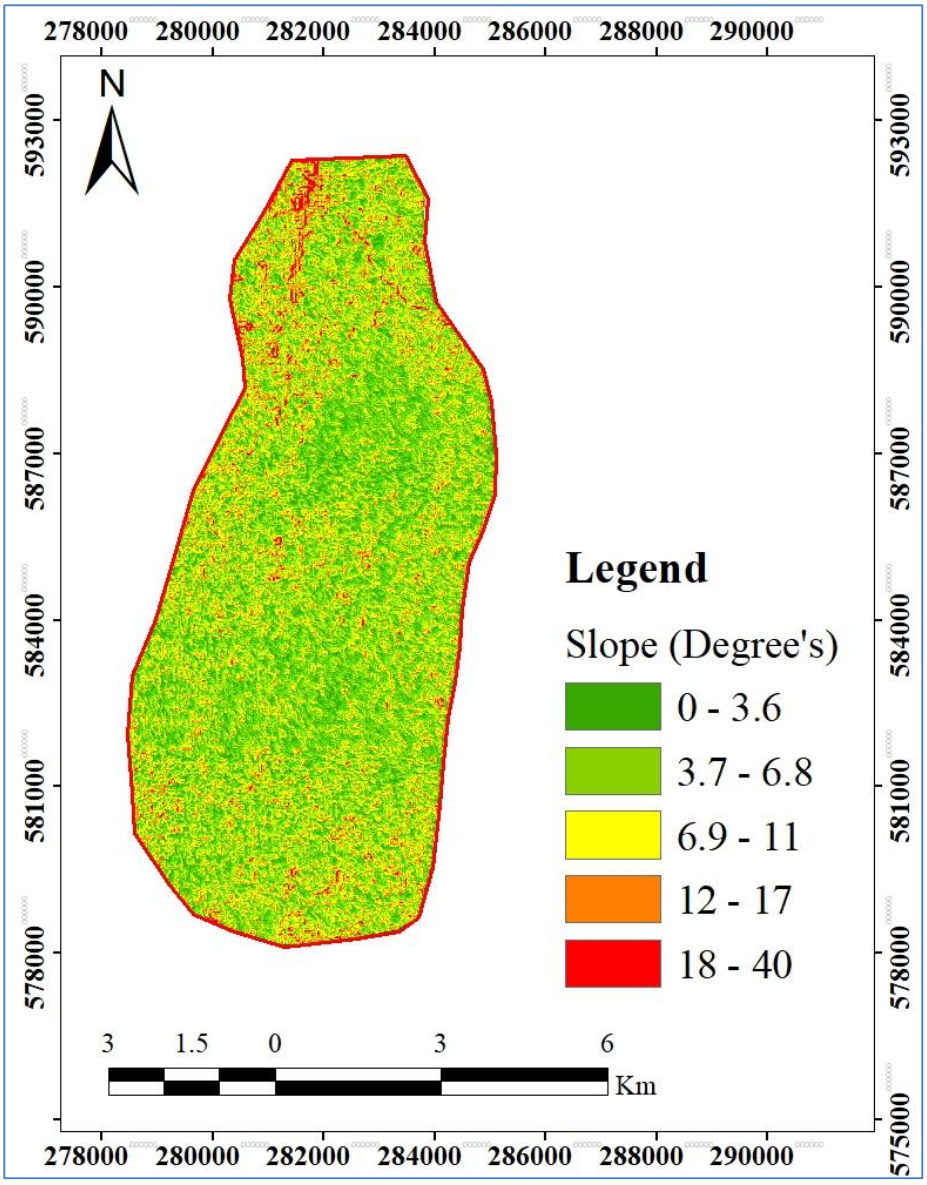
278000
280000
282000
284000
286000
288000
290000
N
593000
590000
587000
584000
581000
578000
575000
Legend
Slope (Degree's)
0 - 3.6
3.7 - 6.8
6.9 - 11
12 - 17
18 - 40
3
1.5
0
3
6
Km

Appendix C: 100 years flood velocity vector

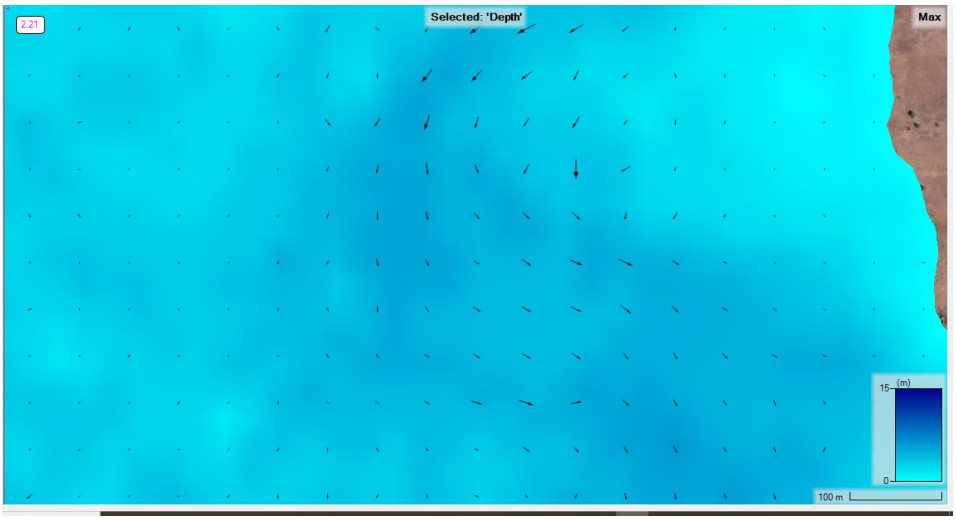

Appendix D: flood hydrograph for different return periods from HEC HMS model

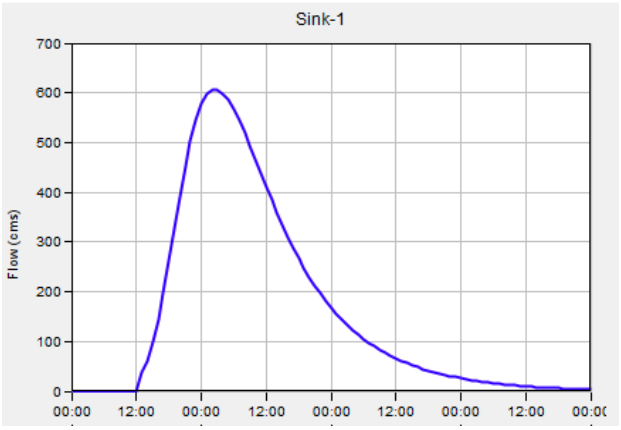

100 years flood hydrograph

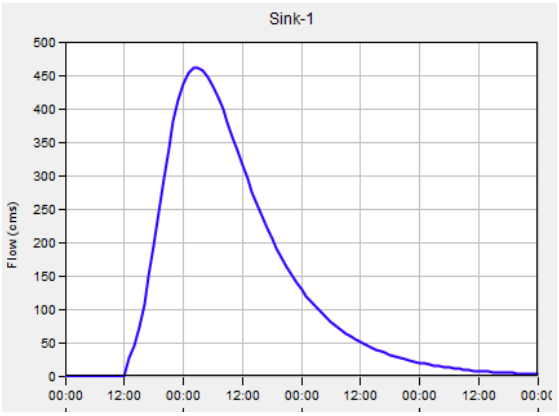

50 years flood hydrograph

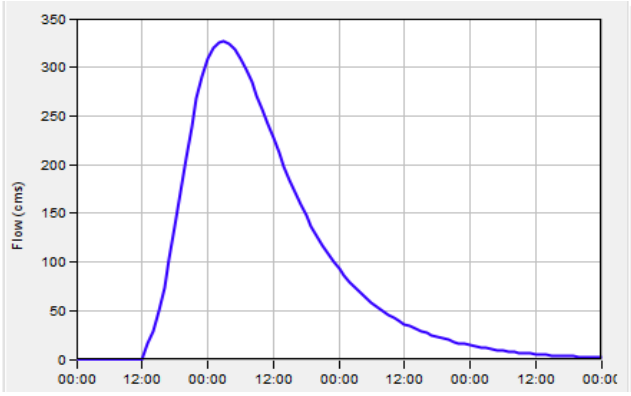

25 years flood hydrograph

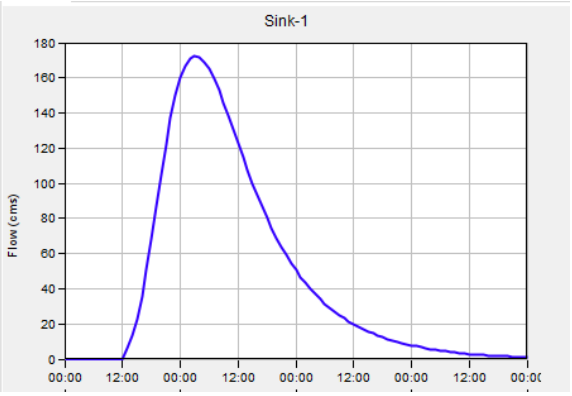

10 years flood hydrograph

Appendix E: Water surface Elevation

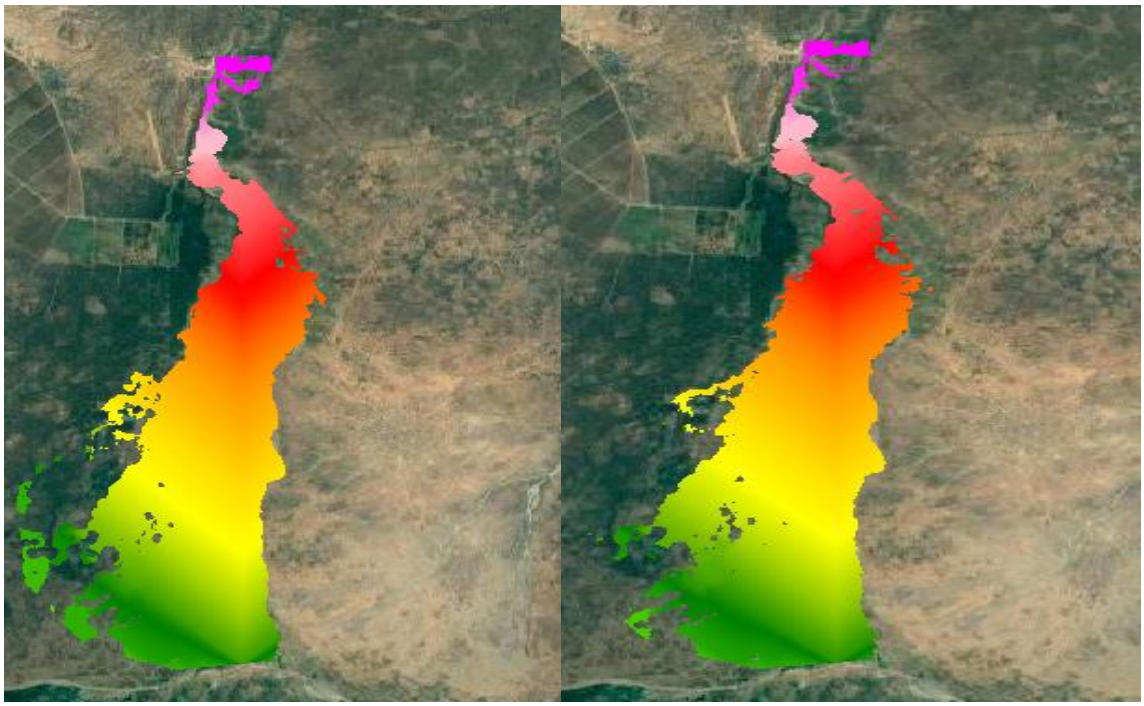

100 years WSE

50 years WSE

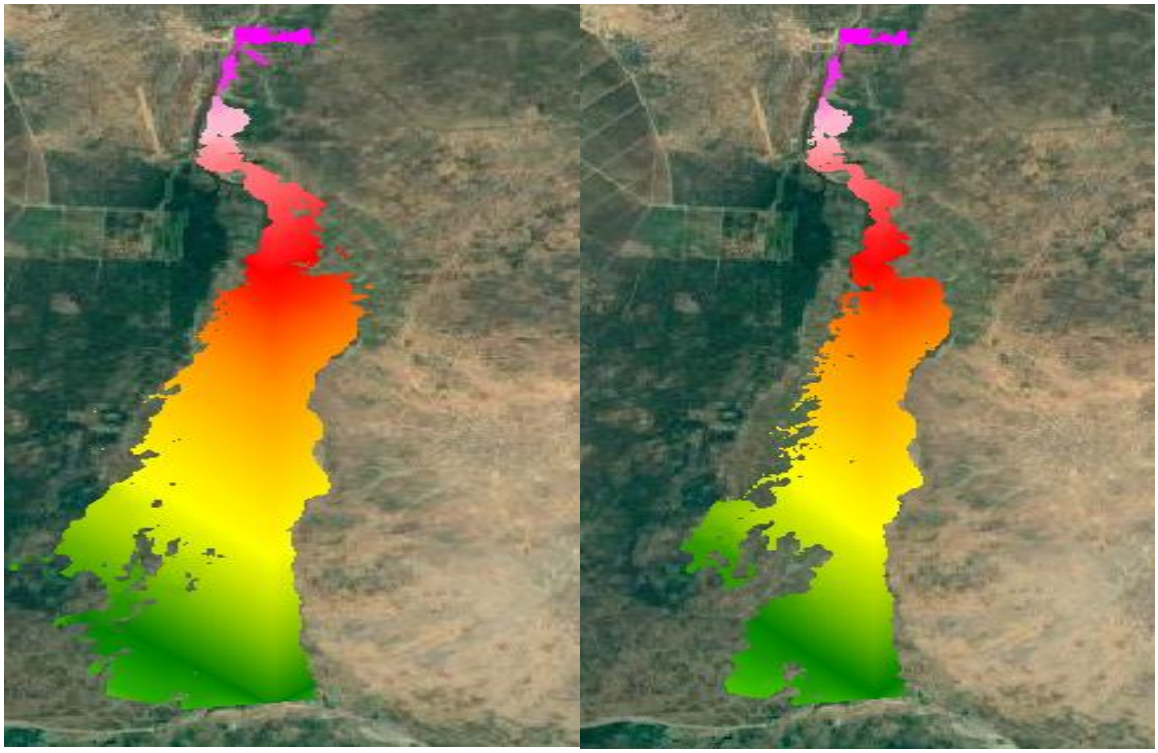

25 years WSE

10 years WSE

Appendix F: 100 years flood inundation below Weito bridge